Role of Jet Temperature in Correlating Jet Noise

K. Viswanathan* and M. J. Czech†

The Boeing Company, Seattle, Washington 98124-2207

DOI: 10.2514/1.35718

The correlation of jet noise spectra, obtained at various jet velocities, has practical relevance; the description and the characterization of the spectral characteristics as functions of the jet operating conditions continue to be of interest. Numerous formulations have been proposed in the last three decades. Recently, new scaling laws, which explicitly identify the jet temperature ratio as an independent controlling parameter, have been developed. Excellent collapse of the spectra from jets at constant stagnation temperature ratios over the entire frequency range was demonstrated. With a newly acquired database at a fixed static temperature ratio, a thorough investigation of the role of static and stagnation temperature ratios in correlating jet noise is carried out. Similar excellent collapse of the spectra is obtained with the static temperature ratio as the independent parameter. Most of the past theoretical studies have relied on Tanna's database to provide the justification for their formulations. A careful assessment of the quality of Tanna's data, both at unheated and heated conditions, has been made through direct comparison with the current data and the use of the current scaling laws. It is established unambiguously that the high-frequency portion of the spectra from unheated jets at all subsonic Mach numbers has elevated levels due to noise contamination. The affected frequency range and the magnitude of the contamination are functions of the Mach number. Even spectra from heated jets at lower temperature ratios but at high subsonic Mach numbers are corrupted; Tanna's data show incorrect spectral trends and are therefore unreliable. It is clearly shown that there is no change in spectral shape due to heating a jet at fixed low jet velocity, contrary to past belief. Thus, there is no experimental basis for many of the theoretical models that identify multiple sources of jet noise at 90 deg. Finally, the scaling law proposed here with either temperature ratio is simple, elegant, and does not contain any adjustable constants whatsoever.

Nomenclature

A	=	nozzle exit area
AA	=	atmospheric attenuation, dB/ft
A_1, B, C	=	multiplicative functions with complicated temperature dependence
a	=	speed of sound in ambient medium
D	=	nozzle diameter
D_m	=	modified Doppler factor
F	=	spectrum function; depends on angle, Strouhal number, and temperature ratio
f	=	frequency, Hz
M	=	jet Mach number
n	=	velocity exponent
p, q	=	exponents of empirical constants α and β
r	=	radial distance
St	=	Strouhal number, fD/V_j
S_m	=	modified Strouhal number
T_j	=	jet static temperature
T_s	=	source temperature
T_t	=	jet stagnation temperature
U, V_j	=	jet velocity
U_c	=	convective velocity
α, β	=	empirical constants
θ	=	inlet angle

Subscripts

a	=	ambient conditions
j	=	jet conditions
s	=	source conditions

I. Introduction

THE correlation of jet noise spectra, obtained at various jet velocities, has practical relevance and has therefore attracted considerable attention in the past several decades. The description and the characterization of the spectral characteristics as functions of the jet operating conditions continue to be of interest. There have been numerous attempts in the past to correlate spectra from heated and unheated jets using a variety of formulations; see [1–8]. A review of all the scaling formulations based on the classical jet noise theory is provided in Sec. III.B in [9]. The main ideas are summarized here. Most of the classical formulations have relied on the acoustic analogy, together with other theoretical considerations. In many of these approaches, scaling laws for jet noise were first developed for a radiation angle of 90 deg, where convection and other effects are negligible. Typically, the chosen form for the intensity or the overall sound pressure level (OASPL) was assumed to be

$$I_{90} \propto A_1(V_j/a)^8 + B(V_j/a)^6 + C(V_j/a)^4 \qquad (1)$$

A_1, B, and C are complicated functions of the temperature ratio and the functional forms depended on the assumptions invoked, with several empirical factors introduced; V_j is the jet velocity, and a is the ambient speed of sound. The three source terms represent contributions from quadrupoles, dipoles, and monopoles, respectively. Some researchers proposed that the sources were correlated while others maintained that the sources were not coherent. In some scaling formulations, only the quadrupole and dipole terms were present; in certain others, the quadrupole and monopole terms were included. The value of the velocity exponent for the quadrupole term was also taken to be 7.5 instead of 8. As pointed out in [9], none of these formulations produces spectral collapse even at a radiation angle of 90 deg, thereby necessitating the expediency for the functional dependences and empirical constants to vary with Strouhal number (frequency) at a given radiation angle. The situation gets murkier at other radiation angles, especially in the peak radiation sector in the aft quadrant. The notion of moving sources led to the idea of convective amplification for noise radiated to the aft angles, with the frequency suitably corrected for Doppler shift. All the theories were based on the premise that it is possible to predict the spectra at any aft angle, with a given shape at 90 deg. At other

radiation angles, the spectral shape is modified to account for effects due to source convection and flow/acoustics interaction. Though the shortcomings with these approaches vis-à-vis experimental data were recognized in the early 1970s, no reliable scaling method emerged; see [9] for more details.

Recently, Viswanathan [9–12] developed new scaling laws that explicitly identified and recognized the jet temperature ratio, along with the acoustic Mach number (V_j/a), as an independent parameter. Specifically, 1) the variation of the overall sound power level with jet velocity has a weak dependence on jet stagnation temperature ratio, and 2) the variation of the overall sound pressure level with velocity at every radiation angle is a function of the jet stagnation temperature ratio. Very good collapse of the spectra measured with nozzles of different diameters and Mach numbers, but at a fixed jet stagnation temperature ratio, was demonstrated over the entire frequency range for all the radiation angles in [9–12]. With a detailed analysis of the spectra in the aft angles, it was shown that the Strouhal number without the Doppler correction is the right choice for normalizing frequency. Therefore, there is no experimental evidence for the idea of moving sources and convective amplification. The new scaling formulation for the turbulent mixing noise spectra at any radiation angle may be written as

$$\text{SPL}(\theta, St) = F(\theta, St, (T_t/T_a))[V_j/a]^n, \qquad n = n(\theta, T_t/T_a) \quad (2)$$

The sound pressure level (SPL) per unit area (or area-normalized SPL) at an arbitrary fixed distance is given by the product of a spectrum function and the velocity ratio raised to the velocity exponent n. The spectrum function F and exponent n, at a particular angle and temperature ratio, are obtained from experimental measurements. When the parameter $[\text{SPL} - 10^*\log_{10}(A/A_{\text{ref}}) - 10^*n^*\log_{10}(V_j/a)]$ for one-third-octave spectra or $[\text{SPL} - 10^*\log_{10}(A/A_{\text{ref}}) - 10^*n^*\log_{10}(Vj/a) - 10^*\log_{10}(D/V_j)]$ for narrowband spectra are plotted against the Strouhal number, a master spectral shape results for every angle and every temperature ratio. A is the nozzle exit area and A_{ref} is a reference area, which is taken here to be one square inch for convenience. This is the aforementioned spectrum function $F(\theta, St, T_t/T_a)$. The velocity exponent n has a unique value and is calculated from the measured overall sound pressure levels at each angle, from jets of different V_j/a, but fixed jet temperature ratio.

The jet stagnation temperature ratio (T_t/T_a) was taken to be the independent parameter for scaling spectra in [9–12]. However, the possibility that the jet static temperature ratio (T_j/T_a) could be equally suitable was mooted and left open in [9]. In Sec. VI of [9], this issue was examined in cursory detail, using selected test points at constant static temperature ratios from the database of Tanna et al. [13,14]. An in-depth investigation of the choice of the stagnation and static temperature ratios in correlating jet spectra using new data is carried out here. There are two comprehensive databases on jet noise, though several experimental programs have been undertaken in many laboratories both in Europe and the United States. The first one is due to Tanna et al. [5,13,14], which has been used extensively in the development and refinement of theoretical models. The second is the more recent one of Viswanathan [9–12]. A critical assessment of the quality of Tanna's data is performed. Because many of the theoretical models are based on the trends observed in Tanna's data, the validity of the theoretical models and the scaling laws derived using the data is also examined in this study.

II.   Experimental Database

A supplemental database, wherein the jet static temperature ratio is held constant, has been recently created. As before, the aeroacoustic test was carried out at Boeing's Low Speed Aeroacoustic Facility. Detailed descriptions of the test facility, the jet simulator, the data acquisition and reduction process, etc., may be found in [9–12]. For the sake of completeness, a brief overview is provided here. Brüel & Kjær quarter-inch type 4939 microphones are used for free-field measurements. The microphones are set at normal incidence and without the protective grid, which yields a flat frequency response up

to 100 kHz. Typically, several microphone arrays are used; these arrays are at a constant sideline distance of 15 ft (4.572 m) from the jet axis and on a polar arc of 25 ft (7.62 m). Very fine narrow band data with a bin spacing of 23.4 Hz up to a maximum frequency of 88,320 Hz are acquired and synthesized to produce one-third-octave spectra, with a center band frequency range of 200–80,000 Hz.

Aeroacoustic data have been acquired at three static temperature ratios (T_j/T_a) of 2.0, 2.5, and 3.0. The nozzle pressure ratio (NPR) was varied systematically to produce jets with Mach numbers of 0.4, 0.5, 0.6, 0.7, 0.8, 0.9, and 1.0 at each jet temperature. Thus, data were acquired over a wide range of jet velocities at each fixed temperature ratio. It is well known that the jet velocity (or the velocity normalized by the ambient speed of sound, V_j/a) is a key parameter in turbulent mixing noise. Table 1 shows the test conditions and the range of the velocity ratios of the selected test matrix. Many concerns with the instrumentation system and the proper steps that would lead to accurate measurements at the higher frequencies are discussed by Viswanathan [15].

Recall that measurements were made over a range of V_j/a at five constant stagnation temperature ratios of 1.0, 1.8, 2.2, 2.7, and 3.2 in the original database. An examination of Table 1 reveals that the stagnation temperature ratio varies over a range of 3.09–3.51, when the static temperature ratio is held constant at 3.0 and the NPR is varied. Additional data have been acquired at two constant stagnation temperature ratios as well: one at 3.14 (approximately the lowest value), and the other at 3.51 (the highest value). Thus, a comprehensive set of data over a wide range of V_j/a at constant stagnation and static temperature ratios from ∼3–3.5 has been generated. Table 2 provides the new test points at constant stagnation temperature ratios.

The as-measured data are corrected to a common (arbitrary) distance of 20 ft (6.096 m) from the center of the nozzle exit (coordinate system with origin at the center of the nozzle exit) and lossless or standard-day conditions: an ambient temperature of 77°F (298K) and a relative humidity of 70%. When lossless spectra are considered, the spectral levels just move up (or down) when the observer distance is reduced (or increased). Therefore, the choice of 20 ft has no special significance. The atmospheric attenuation coefficients are obtained from the method found in Shields and Bass [16]. The standard practice of converting the as-measured data to lossless form and then propagating the spectra to a common distance (of 20 ft) while accounting for the atmospheric absorption at standard-day conditions has been adopted. Implicit in this process is the assumption of linear propagation, with the sound pressure level obeying the $1/r^2$ dependence. The normalization process may be written as follows:

$$\text{SPL}_{(20\,\text{ft})} = \text{SPL}_{\text{measured}} - 10\log_{10}(20/R)^2 + R[AA_{(\text{test day})}]$$
$$- 20[AA_{(\text{std day})}] \quad (3)$$

where R is the distance (in feet) of the microphone from the origin of the coordinate system, and $[AA]$ are the atmospheric absorption coefficients (which are frequency dependent) per foot. Equation (3) provides spectra corrected to standard-day conditions; for lossless data, the last term in this equation is omitted. The accuracy of the weather corrections and the suitability of the different proposed methods have been evaluated by Viswanathan [12]; it was shown that the method found in Shields and Bass [16] was the best at the higher frequencies of interest in the model scale tests.

III.   Results and Discussion

A.   Overall Levels

First we examine the variation of the overall power level (OAPWL) with the velocity ratio, V_j/a. Figure 1 shows the distribution for all the test points in Table 1; also shown is the straight line that corresponds to the V^8 variation. There is seemingly good agreement of the trend observed for the different test points with the theoretical curve; this trend has been noted for the past several decades. In Fig. 2, the data are grouped according to the fixed static

Table 1   Test conditions at three constant static temperature ratios

NPR	T_j/T_a	T_t/T_a	V_j/a	T_j/T_a	T_t/T_a	V_j/a	T_j/T_a	T_t/T_a	V_j/a
1.12	2.0	2.06	0.57	2.5	2.58	0.64	3.0	3.09	0.70
1.19	2.0	2.10	0.71	2.5	2.62	0.80	3.0	3.14	0.88
1.28	2.0	2.14	0.86	2.5	2.67	0.96	3.0	3.19	1.05
1.39	2.0	2.19	0.99	2.5	2.73	1.11	3.0	3.26	1.22
1.52	2.0	2.24	1.13	2.5	2.79	1.26	3.0	3.33	1.38
1.69	2.0	2.31	1.27	2.5	2.87	1.42	3.0	3.42	1.55
1.89	2.0	2.38	1.41	2.5	2.95	1.58	3.0	3.51	1.72

temperature ratios with a least-squares curve fit for each fixed jet static temperature ratio; the curves have also been spaced apart for better visual effect. A weak dependence of the OAPWL with temperature emerges; the value of the velocity exponent decreases as the jet static temperature ratio is increased. These trends are consistent with those observed at fixed stagnation temperature ratios Sec. III.D of [10]. Thus, it is clear that the OAPWL does not follow exactly the V^8 law. For the static temperatures considered here, the value of the velocity exponent decreases from 8.1 for $T_j/T_a = 2.0$ to 7.78 for $T_j/T_a = 3.0$. This decrease is comparable to the exponent values for jets at fixed stagnation temperature ratios: 8.34 for $T_t/T_a = 2.2$ and 7.98 for $T_t/T_a = 3.2$. It is now established that the OAPWL has a weak dependence on jet temperature ratio, regardless of the choice of the stagnation or the static temperature ratio. The classical value of 8 for the exponent is not strictly valid.

B.   Scaling of Spectra

We now turn our attention to the scaling of spectra from jets at constant T_j/T_a. The velocity exponents for the three fixed static temperature ratios at each radiation angle are calculated from the least-squares fits of the OASPL. Figure 3 shows the variation of the calculated velocity exponent with angle. The values of the exponent are low, between ~5 and ~6, at the lower radiation angles. As we move to the aft angles, the values start to rise and an exponent of ~9.2 is reached at 150 deg for the case of $T_j/T_a = 2.0$. At a given angle, the exponent is typically lower for the hotter jet. The trends are very similar to those seen for jets at constant stagnation temperature ratios; see Fig. 16 in [9] for the variations of the velocity exponent at the original five constant stagnation temperature ratios.

Next we demonstrate that the calculated velocity exponents indeed collapse the spectra at all radiation angles. Figure 4 shows the normalized spectra at 90 deg for jets with $T_j/T_a = 2.0$; there is excellent collapse over the entire Strouhal number range (raw frequency range of 200–80 kHz) for the six Mach numbers shown. Figure 5 shows a similar plot with the normalized spectra at two static temperature ratios of 2.0 and 3.0 at 100 deg. In addition to the excellent collapse at each fixed temperature ratio, the normalized spectral shapes are almost identical for the two temperatures. Note that the values of the velocity exponents are different, however. It was shown by Viswanathan [10,17] that the spectra from heated jets at the lower radiation angles have a universal shape and conform to the fine-scale similarity spectra of Tam et al. [18] regardless of the jet Mach number and temperature. This result is once again confirmed by the spectral collapse shown here and in [9,11].

Special care is needed when collapsing spectra at larger aft angles, as discussed in great detail in Sec. IV of [11] with reference to jets at constant stagnation temperatures. The same issues are pertinent and important for jets at constant static temperature ratios as well. An added complication arises for convectively supersonic jets due to nonlinear propagation effects. Viswanathan [19] first reported on this phenomenon of nonlinear propagation for subsonic heated laboratory jets and identified the convective Mach number as a reliable indicator for predicting the onset of nonlinear effects. Specifically, when the convective Mach number exceeds unity, there is a transfer of energy to the higher frequencies, manifested by increased spectral levels. This agglomeration is independent of the overall sound amplitude and is controlled mainly by the convective

Mach number; see [11,12] for further details. Another sample collapse, at an angle of 120 deg, is shown in Fig. 6; the static temperature ratio is 3.0 for this case. Again, there is excellent collapse over the entire Strouhal number range for the lower three Mach numbers of 0.6, 0.7, and 0.8. At the upper two Mach numbers of 0.9 and 1.0, the spectral levels at the higher frequencies have elevated amplitudes; the magnitude of the increase is seen to be higher, roughly ~6 dB at a Strouhal number of ~8, for the $M = 1.0$ jet. It was clearly shown in [12] that the increase in level is directly proportional to the propagation distance. It was also established that jets with velocities greater than ~1600 ft/s (490 m/s), or $V_j/a > \sim 1.43$, would experience nonlinear propagation effects. An examination of Table 1 indicates that the values of V_j/a are 1.55 and 1.72, respectively, for the $M = 0.9$ and 1.0 jets.

The analyses carried out in Sec. IV.C of [11] indicated that the nonlinear effects are confined to an angular sector of $\geq \sim 130$ deg for jets with $V_j/a \approx 1.64$. The elevated levels at the higher frequencies in Fig. 7 imply that nonlinear effects are manifested at lower inlet angles when the jet velocity is progressively increased, thereby extending the angular range in the aft quadrant where these effects need to be considered. Figure 7 shows the normalized spectra at the same radiation angle of 120 deg for the jets at a constant stagnation temperature ratio of 3.51 shown in Table 2. The nonlinear effects are again clearly seen for the $M = 1.0$ jet; further, there is excellent spectral collapse for the subsonically convective jets. It is verified that this is actually the case with Fig. 8, which shows the normalized spectra at a slightly lower stagnation temperature ratio of 3.2. Excellent collapse of the spectra from jets at five different Mach numbers is observed at all frequencies. Again, a single exponent provides this level of collapse.

Figure 9 shows the spectra from both sets of data from Figs. 6 and 7 in the same plot. Interestingly, there is very good overlap regardless of which temperature ratio (and the corresponding velocity exponent) is used. Figure 10 shows the normalized spectra at two static temperature ratios of 2.0 and 3.0 at a further aft angle of 130 deg. The normalized spectral shape for the hotter case has a sharper peak and a faster roll off at the higher frequencies; a similar trend is seen for jets at different constant stagnation temperature ratios.

Therefore, it can be concluded that the spectra normalized using either temperature ratio yield the same consistent characterization. The trends observed here provide added testament to the suitability of the form of the scaling relation proposed in Eq. (2). A close examination of Figs. 6 and 7 reveals that the spectral collapse is tighter for the jets at constant stagnation temperature ratios (also seen in Fig. 8 and the examples shown in [9,11]). Perhaps the choice of the stagnation temperature ratio is slightly better than the static temperature ratio for correlating jet noise, but not by an appreciable

Table 2   Test conditions at two additional constant stagnation temperature ratios

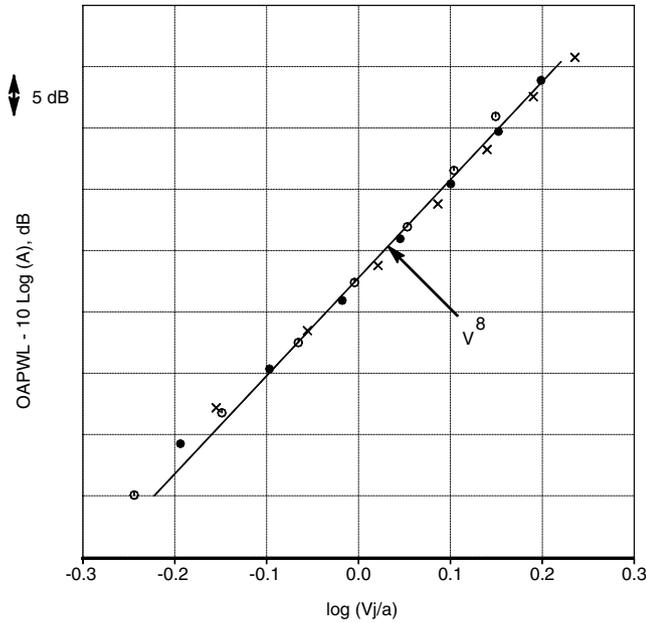| NPR	T_t/T_a	T_j/T_a	V_j/a	T_t/T_a	T_j/T_a	V_j/a
1.19	3.14	3.00	0.88	3.51	3.36	0.93
1.28	3.14	2.94	1.04	3.51	3.30	1.10
1.39	3.14	2.88	1.19	3.51	3.23	1.26
1.52	3.14	2.82	1.34	3.51	3.16	1.42
1.69	3.14	2.74	1.49	3.51	3.08	1.57
1.89	3.14	2.67	1.63	3.51	2.99	1.72

Fig. 1 Variation of the overall power level with the normalized jet velocity; all temperature ratios and jet Mach numbers in Table 1. Straight line: V^8 variation.

degree. We defer discussion of the form proposed in Eq. (1) until Sec. III.E. The extension of the new scaling laws to dual-stream jets is not straightforward. There are several sources: the inner shear layer between the primary and secondary jets, the outer shear layer between the secondary jet and the ambient air (either static or with a flight stream), and the fully developed jet farther downstream. The contribution from each source depends on the jet operating conditions (the NPR and temperature ratio in the two streams) and the nozzle area ratio. An experimental database with parametric variation of the different thermodynamic conditions has been generated. Analyses and development of a prediction method with the different sources modeled as equivalent single jets are underway. The current scaling laws will play a direct role in the prediction of noise from the equivalent single jets.
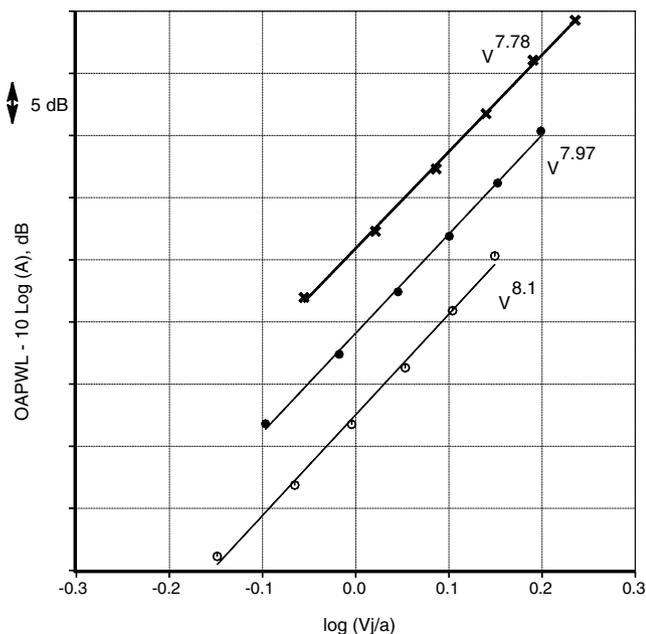
Fig. 2 Variation of the overall power level with the normalized jet velocity. Open circles: $T_j/T_a = 2.0$; closed circles: $T_j/T_a = 2.5$; x: $T_j/T_a = 3.0$; solid lines: least-squares fits through data. Curves have been spaced apart for better visual effect.
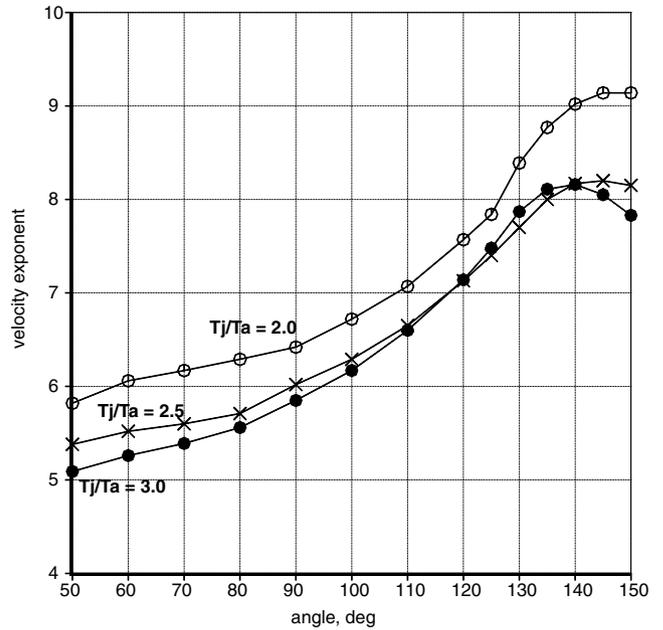

Fig. 3 Velocity exponent for various angles and constant jet static temperature ratios.

C. Assessment of Tanna's Database

1. Unheated Jets

Almost all the theories and scaling methodologies for jet noise developed in the past 30 years have been based on the experimental database of Tanna et al. [5,13,14]; these data will be simply referred to as Tanna's data hereafter. Many characteristics of jet noise, such as the effect of heating, the noise of jets at constant jet velocity, the observation of two master spectral shapes, etc., have been derived mainly from this database. It is, therefore, à propos to carry out a careful assessment of the quality of Tanna's data and revisit the beliefs derived therefrom. Viswanathan [10,20] examined the quality of the spectral measurements from five different aeroacoustic facilities; it was clearly demonstrated that almost all the past data suffer from varying levels of contamination, from ~2 to ~6 dB depending on the jet operating conditions and radiation angle, due to extraneous noise. Figure 11 shows a direct comparison of three jet
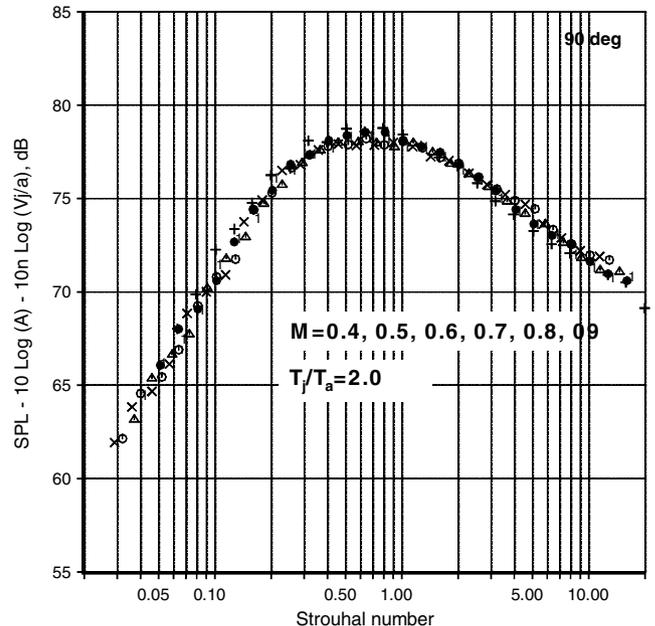

Fig. 4 Normalized spectra at 90 deg for a range of Mach numbers. $T_j/T_a = 2.0$. Velocity exponent $n = 6.42$.
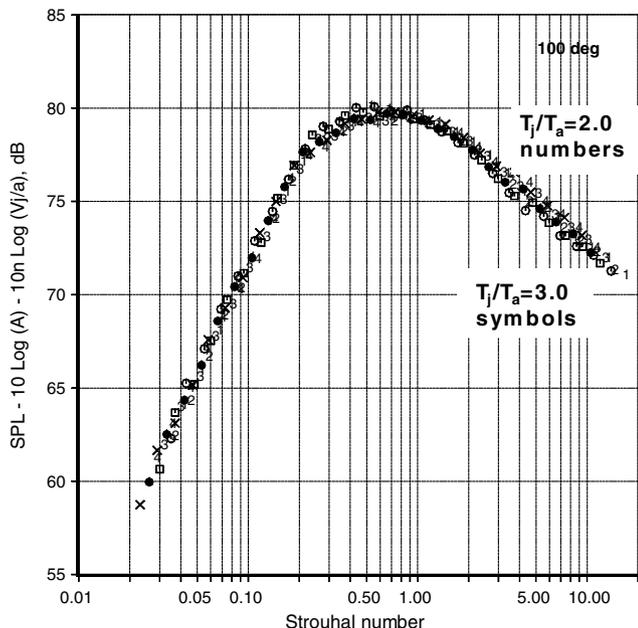
Fig. 5 Normalized spectra at 100 deg for a range of Mach numbers. Numbers: $T_j/T_a = 2.0$, **velocity exponent** $n = 6.72$; **symbols:** $T_j/T_a = 3.0$, **velocity exponent** $n = 6.17$.

Fig. 7 Normalized spectra at 120 deg for a range of Mach numbers at constant stagnation temperature ratio. $T_t/T_a = 3.51$, **velocity exponent** $n = 7.32$.

velocities: $V_j/a = 0.4$, 0.6, and 0.9. The jet Mach numbers correspond to 0.4, 0.62, and 1.0, respectively. The dark symbols denote Tanna's data and the open symbols the current database. The arrows indicate the values of the raw frequencies in hertz in Tanna's measurements. First of all, Tanna's spectral levels are much higher over an extended frequency range, denoting high levels of contamination. The contaminated frequency range is a function of jet velocity: the range and the amplitude of the contamination are more pronounced at lower jet velocity. For instance, at $V_j/a = 0.4$, Tanna's spectrum exhibits higher levels from 2500 (St $\approx$ 1.0) to 40 kHz; the level of contamination is greater than 3 dB for frequencies of $\geq \sim 5$ kHz. From the trends seen in this figure, it is abundantly clear that Tanna's data suffer from substantial contamination over a very wide range of frequencies, starting from as low as $\sim$2500 Hz and extending all the way to 40 kHz at the lower
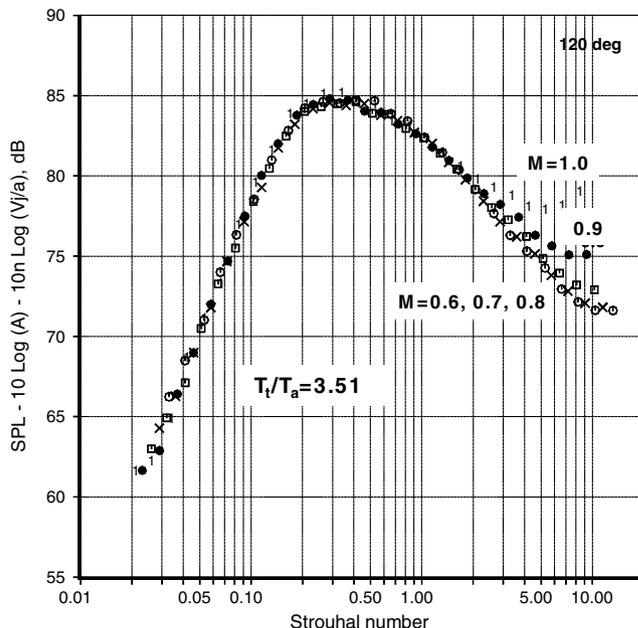
jet velocities. It is also important to recognize that the spectra at all subsonic jet Mach numbers are subject to varying levels of contamination.

2. Heated Jets

The characterization and modeling of the noise from heated jets have attracted tremendous attention from numerous researchers since the early 1970s; see [2–8] for a partial list. Tanna's data provided the underpinning and the justification for most of the theoretical developments. Specifically, experimental evidence for the presence of two noise sources at 90 deg, even though the effects due to convective amplification and refraction are negligible, is due to the seemingly two different spectral shapes observed by Tanna et al. [5]. Figure 6 in [5] is reproduced here as Fig. 12 to aid the following discussion. The effect of temperature on the spectra at a
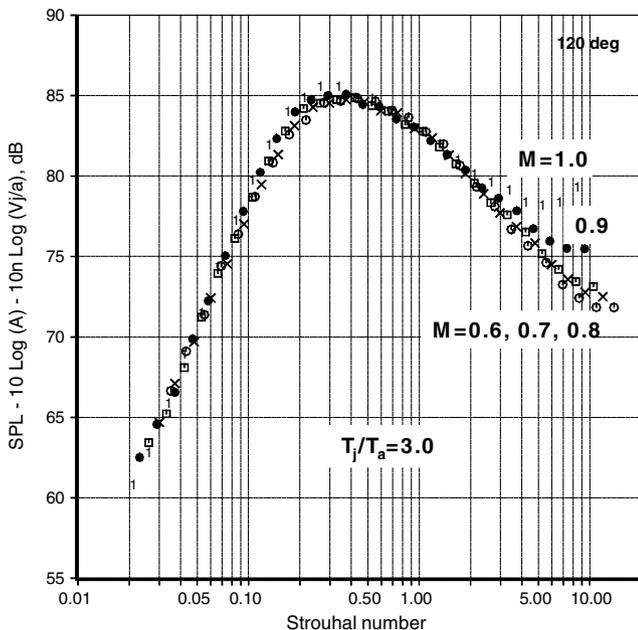

Fig. 6 Normalized spectra at 120 deg for a range of Mach numbers at constant static temperature ratio. $T_j/T_a = 3.0$, **velocity exponent** $n = 7.14$.
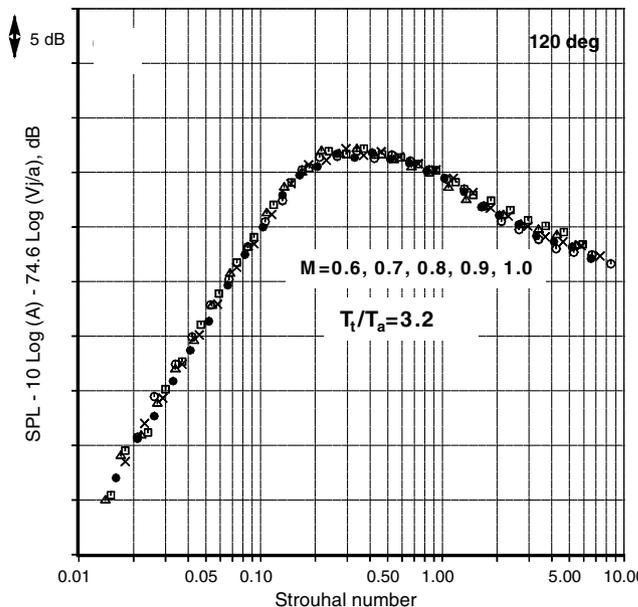

Fig. 8 Normalized spectra at 120 deg for a range of Mach numbers at constant stagnation temperature ratio. $T_t/T_a = 3.2$, **velocity exponent** $n = 7.46$.
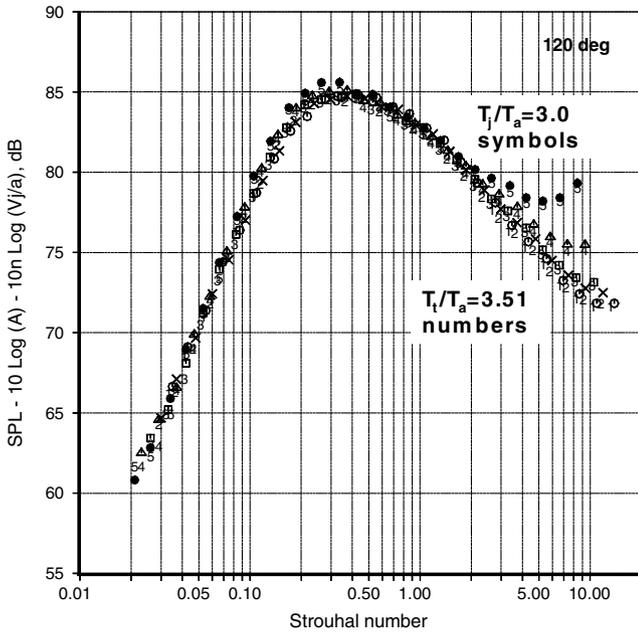
Fig. 9   Normalized spectra at 120 deg for a range of Mach numbers.

Fig. 11   Comparison of data from Tanna [13,14] with current database. Unheated jets at various jet velocities. Dark symbols: Tanna; open symbols: Viswanathan [9,10].

low velocity ($V_j/a = 0.4$) is depicted; Tanna et al. [5] state that "the isothermal jet shows the characteristic broadband spectrum while the effect of elevated temperature clearly is to provide a significant noise increase, particularly in the lower frequencies." Their main conclusion in the abstract is that, at 90 deg, "in general, two sources of noise are apparent, one resulting from the familiar Reynolds shear stress fluctuations and a second attributable to density or temperature fluctuations promoted by the turbulent mixing of streams of dissimilar temperatures."

Another means employed for uncovering the relative importance of these two sources was through the investigation of the noise from jets at fixed V_j/a. As noted in Viswanathan [10], it should be kept in mind that jets at fixed velocity are not operated at constant thrust. The spectra from these jets can not be normalized for constant thrust, as indicated by an examination of the thrust equation. Once the thermodynamic conditions, the nozzle pressure ratio, and the jet stagnation temperature ratio are chosen to yield a desired jet velocity,

the only free parameter available to change thrust is the nozzle diameter. Therefore, nozzles of increasing diameters would be required as the jet temperature is increased and the nozzle pressure ratio decreased to maintain constant V_j/a. This practice is seldom adopted. The main purpose of these measurements, of course, is to evaluate the effect of decreased jet density with heating on the radiated noise.

A typical result, Fig. 7 in Tanna et al. [5], at a medium velocity with $V_j/a = 0.8$ is reproduced here as Fig. 13. The spectra from an unheated jet and five heated jets at 90 deg are shown; the static temperature ratios span a range of 0.865–2.877. The spectral levels start to diverge for frequencies greater than ~4 kHz; as the jet temperature is increased at this fixed V_j/a, there is a progressive reduction in the amplitude at the higher frequencies. This reduction becomes more pronounced with increasing frequency and reaches ~8 dB between the unheated case and the jet with the highest temperature at 40 kHz. Further, note that the difference in levels is ~7 dB even among the heated jets.

Let us reevaluate the validity of the data and the associated theories with the database of Viswanathan [9,10]. Figure 14 shows a comparable plot, at $V_j/a = 0.8$ and at 90 deg, from a nozzle with a 2.45 in. (6.17 cm) diameter. The spectrum for the unheated jet is
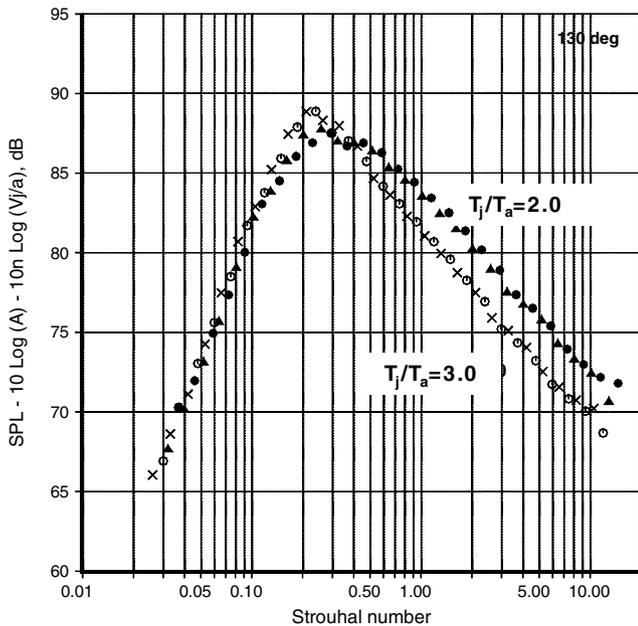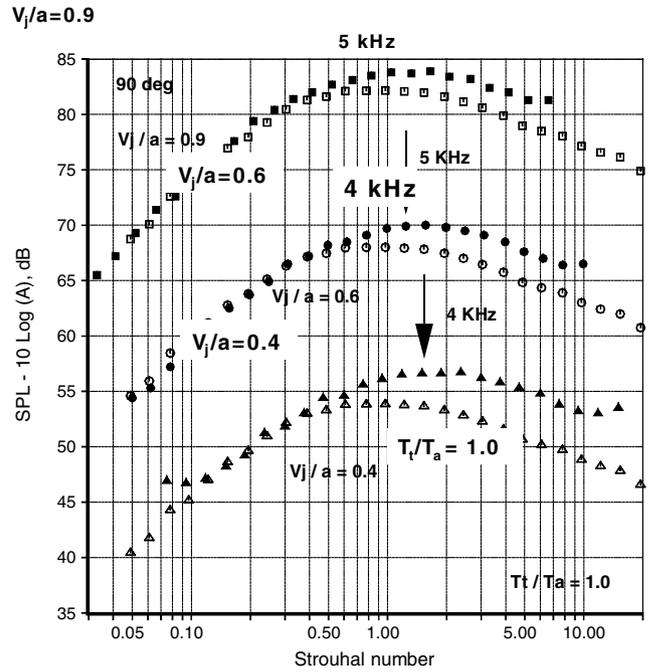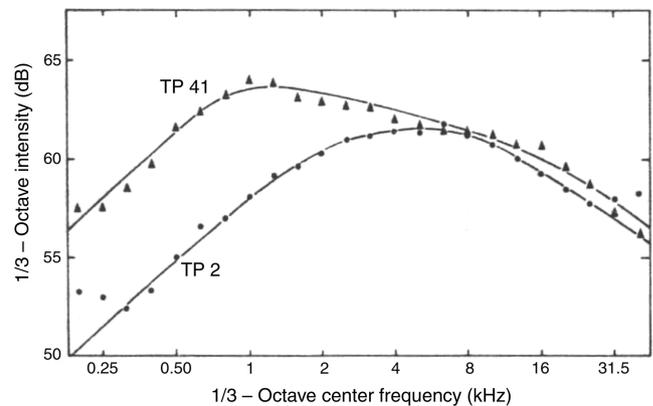

Fig. 10   Normalized spectra at 130 deg from jets at two constant static temperature ratios. Open symbols: $T_j/T_a = 3.0$; closed symbols: $T_j/T_a = 2.0$.

Fig. 12   Effect of temperature on jet noise at low velocity ($V_j/a = 0.4$). Closed circles: $T_j/T_a == 0.961$ (unheated); triangles: $T_j/T_a = 2.88$. Figure 6 in Tanna et al. [5].
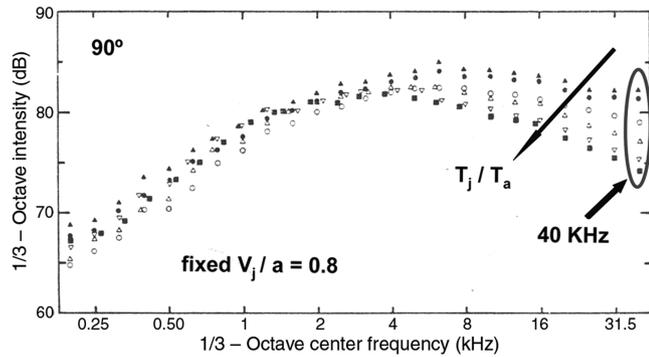
Fig. 13 Effect of temperature on jet noise at medium velocity ($V_j/a = 0.8$). $T_j/T_a = 0.865, 0.977, 1.408, 1.764, 2.271$, and 2.877. Figure 7 in Tanna et al. [5].

denoted by the solid circle, and the spectra for the heated jets are denoted by the open symbols. The stagnation temperature ratios cover a range of 1.0–3.05, with a corresponding range for the static temperature ratios of 0.87–2.93. Thus, there is very good overlap between the jet static temperature ratios in the data sets of Tanna and Viswanathan. First of all, the unheated jet has elevated levels over a wide range of higher frequencies. An astonishing feature, in contrast to the trend seen in Fig. 13, is that all the heated jets have the same spectral levels at the higher frequencies. There is tight collapse of the spectra in the frequency range of 5–80 kHz, with slight differences at the lower frequencies. The spectrum from the highest temperature jet is highlighted with the number 2 and a line. The spectral level is higher near the peak and slightly to the left of the peak frequency. At this high temperature, the Reynolds number drops to ∼200, 350, whereas it is ∼1.85×10^6 for the unheated jet. The value of the Reynolds number is greater than ∼291, 300 for all the other cases. As noted by Viswanathan [10], when the Reynolds number is below ∼400, 000, the spectra from heated jets exhibit an "extra hump" in this frequency regime; see [10] for more details.

When the trends observed in Fig. 14 are compared with those from Tanna in Fig. 13, especially the large spread in the spectral levels at the higher frequencies, it becomes clear that the spectra from heated jets are also subject to varying levels of contamination. Perhaps this should not be too surprising given the magnitude of the contamination by rig noise for frequencies ≥ 4 kHz in Fig. 11 for unheated jets.

Direct comparisons of heated jets at high subsonic Mach numbers are shown in Fig. 15. The spectra at 90 deg from jets with $V_j/a =$

1.16 and 1.48 and at 120 deg with $V_j/a = 1.33$ are shown. There is good spectral agreement between the data acquired by Tanna and Viswanathan at both the radiation angles for these high-velocity jets at high jet temperature ratios: $M = 0.77$ and $T_j/T_a = 2.27$, $M = 0.98$ and $T_j/T_a = 2.27$, $M = 0.79$ and $T_j/T_a = 2.86$.

Let us now examine Tanna's spectra at medium and high jet velocities ($V_j/a = 0.8$ and 1.16) but at lower temperature ratios. Figure 16 shows such a comparison with jets at $M = 0.67$ and $T_j/T_a = 1.43$ and $M = 0.97$ and $T_j/T_a = 1.43$. At both conditions, there is good agreement at the lower Strouhal numbers. However, Tanna's spectra have elevated levels at the higher frequencies. Figure 17 shows another comparison at an even higher temperature: $V_j/a = 1.16$, $M = 0.86$, and $T_j/T_a = 1.82$. In this figure, spectra obtained with two different jet diameters of 2.45 and 3.46 in. in the current database are shown; the area-normalized spectra are in good agreement. Again, Tanna's spectrum has elevated levels at the higher frequencies.

Next we examine the noise from jets at a high fixed V_j/a of 1.16 from Tanna's database in Fig. 18. All the jets are heated, with $T_j/T_a = 1.43, 1.82, 2.27$, and 2.86; the corresponding test points are TP20, TP28, TP37, and TP47, respectively. All the spectra have the same levels at the lower frequencies up to a Strouhal number of ∼0.4. At higher frequencies, the spectral levels start dropping as the jet temperature is increased. The difference in amplitude between the two extreme temperatures of 1.43 and 2.86 at the highest frequency of 40 kHz is 7 dB. A comparable plot at a fixed jet velocity of 1.2 from the database of [9,10] is shown in Fig. 19 at the same angle of 90 deg. Six temperature ratios are considered, with $T_j/T_a = 1.43, 1.63, 1.82, 2.01, 2.21$, and 2.79. Again, there is very good overlap of the temperature ratios in the data sets of Tanna and Viswanathan. As seen in Fig. 18, the spectral levels are the same for all T_j/T_a at the lower frequencies, but up to a Strouhal number of ≤ 0.6. At the higher frequencies, there is a progressive reduction in level with heating; at this high V_j/a (=1.2), there is a steady reduction in OAPWL as well, as seen in Fig. 31 in Viswanathan [10], and this trend is consistent with past observations. However, the maximum drop in levels is ∼2 dB, from ∼20 to 80 kHz (St = 3.0–12.0). Contrast this trend with that in Fig. 18, in which the curves spread apart progressively with increasing frequency and reach 7 dB at 40 kHz.

The curve denoted by the dark circle and the line in Fig. 18 corresponds to TP37. As shown in Fig. 15 in the bottom curves, there is good agreement between this spectrum and that from the current database at the same angle of 90 deg. When we consider the observation in Fig. 19 that the difference in spectral levels between
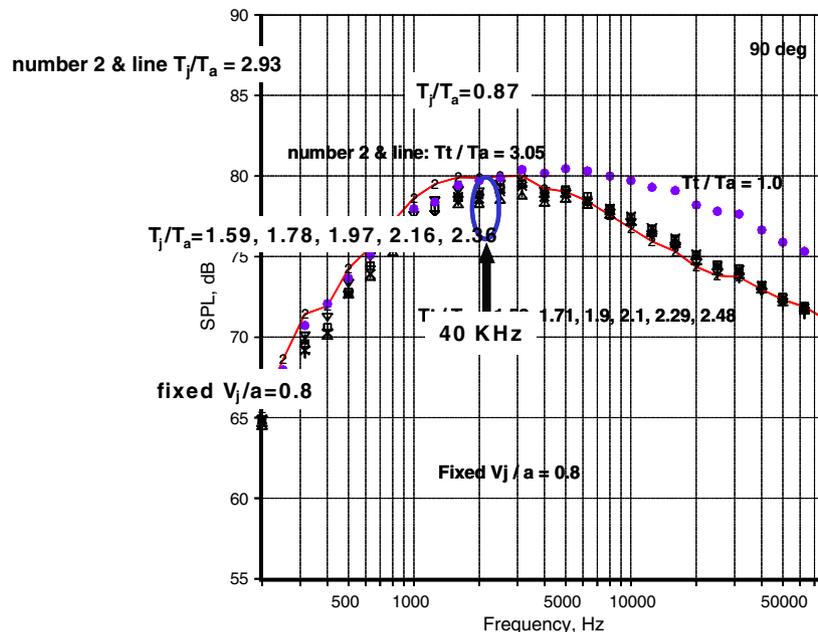

Fig. 14 Effect of temperature on jet noise at medium velocity ($V_j/a = 0.8$). $T_j/T_a = 0.87, 1.59, 1.78, 1.97, 2.16, 2.36$, and 2.93.
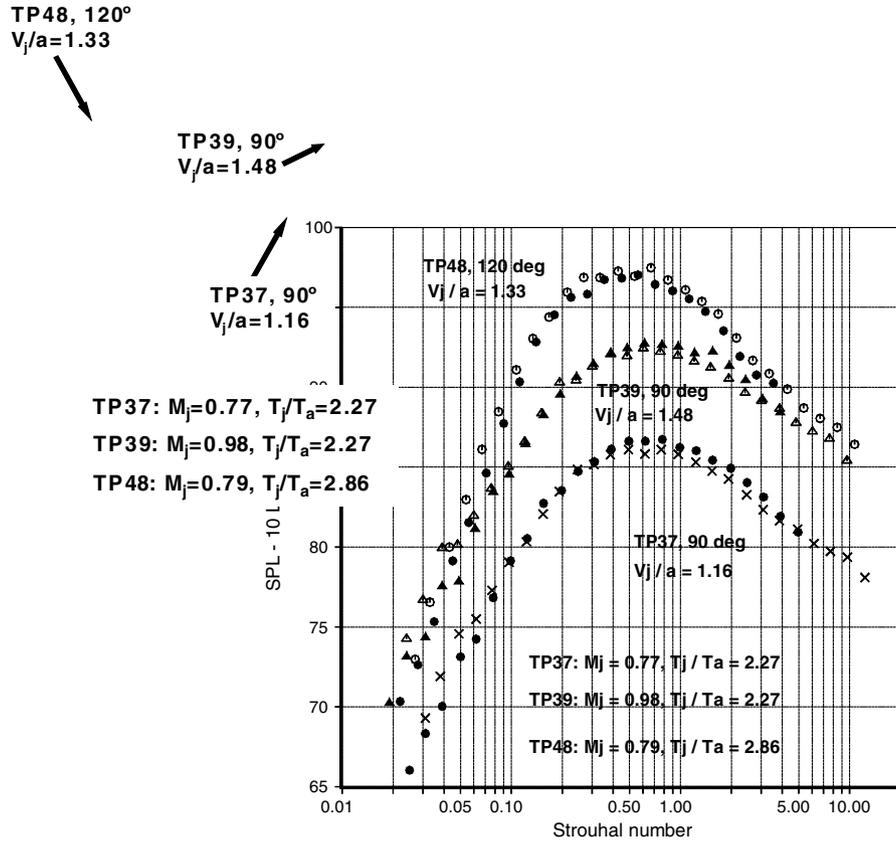
Fig. 15   Comparison of data from Tanna [13,14] with current database. Heated jets at various jet velocities. Dark symbols: Tanna; open symbols: Viswanathan [9,10].

the jets at T_j/T_a of 1.43 and 2.21 is 2 dB, whereas it is 6 dB at 40 kHz in Tanna's data for a similar temperature range of 1.43–2.27, it becomes clear that the jets at the lower temperature ratios in Tanna's database are subject to contamination by rig noise. Note that the jet velocity is high, with $V_j/a = 1.16$.

From the direct comparisons shown in Figs. 16 and 17, and from the trends observed in Figs. 11–19, one can arrive at the following conclusions about Tanna's data:

1) The low-frequency portion of the spectra are accurate for unheated jets for $V_j/a \geq \sim 0.4$.

2) The low-frequency portion of the spectra are accurate for medium- and high-velocity heated jets; it is corrupted for $V_j/a \approx 0.4$, and the lower velocity limit is not known.

3) The entire spectra are of good quality for highly heated jets, with $T_j/T_a \geq 2.27$, at high Mach numbers of $\geq \sim 0.75$.
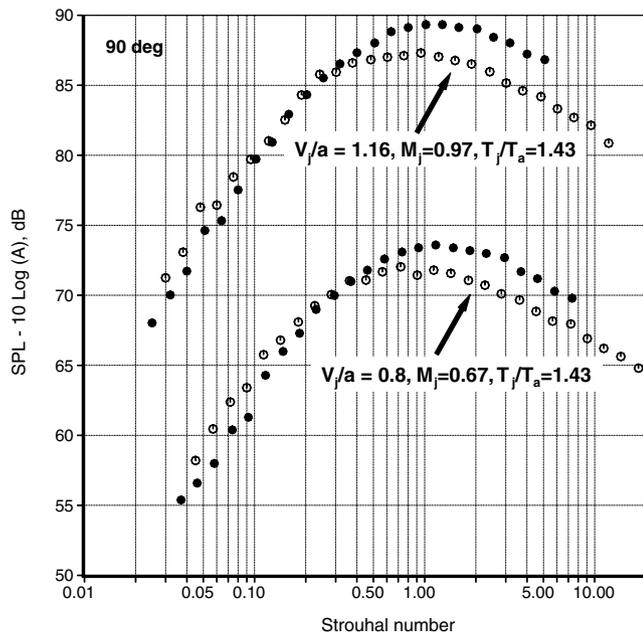

Fig. 16   Comparison of data from Tanna [13,14] with current database. Heated jets at various jet velocities. Dark symbols: Tanna; open symbols: Viswanathan [9,10].
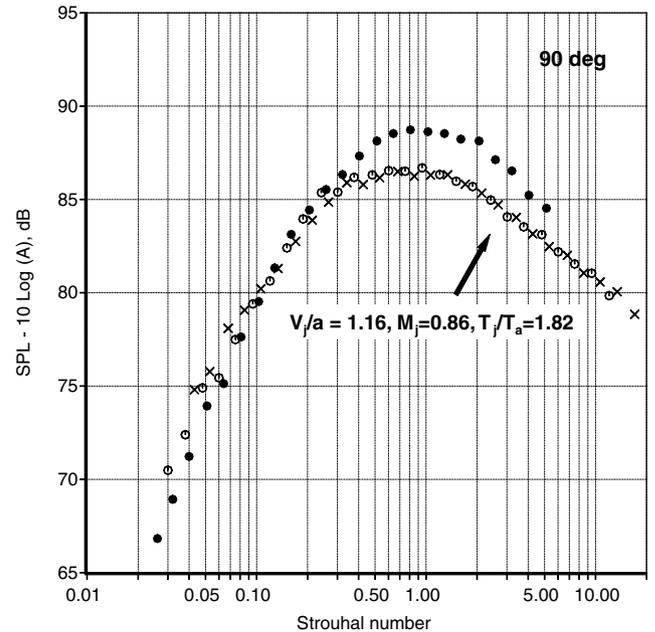

Fig. 17   Comparison of heated jet spectra. Closed circles: Tanna [13,14]; open circles: $D = 2.45$ in.; and x: $D = 3.46$ in. (Viswanathan [9,10]).
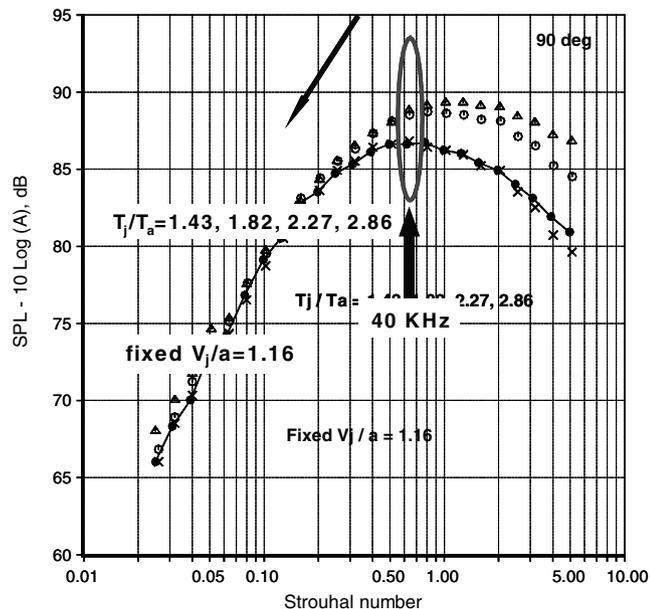
Fig. 18 Effect of temperature on jet noise at a high velocity ($V_j/a = 1.16$). Tanna's data, test points 20, 28, 37, and 47.

4) The levels over a wide frequency range that includes the spectral peak and higher frequencies are contaminated for all unheated subsonic jets up to a Mach number of unity.

5) The range of affected frequencies can be from ~2500 to 40 kHz for unheated jets, depending on jet velocity.

6) There is a high level of contamination even for heated jets up to $T_j/T_a \approx 1.82$ for all jet Mach numbers up to ~0.97.

7) The range of affected frequencies is from ~5000 to 40 kHz for all subsonic heated jets up to $T_j/T_a \approx 1.82$. The magnitude of the contamination is clearly a function of the jet conditions: it can be ~4 dB at the spectral peak and higher frequencies even for heated jets. It is shocking that the level of contamination is so high even for high subsonic (transonic) heated jets.

3. Application of Current Scaling Laws to Tanna's Data

The scaling law represented by Eq. (2) is now applied to Tanna's database, with a typical example shown in Fig. 20. The spectra at
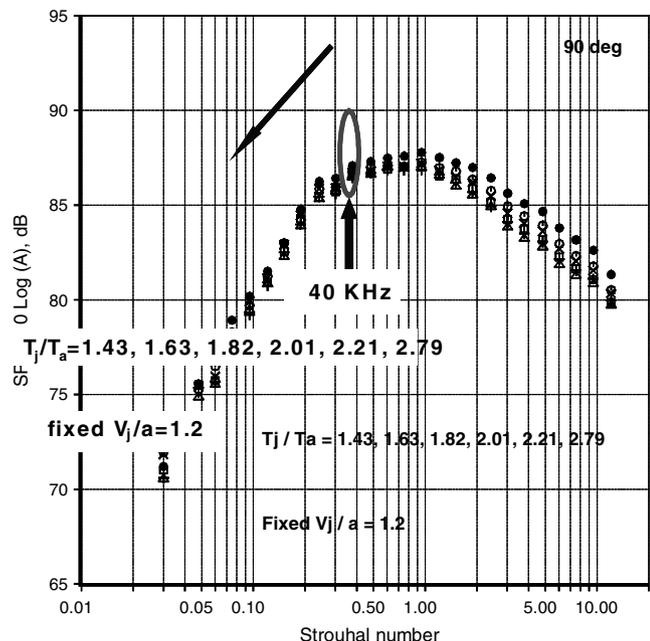

Fig. 19 Effect of temperature on jet noise at a high velocity ($V_j/a = 1.2$).
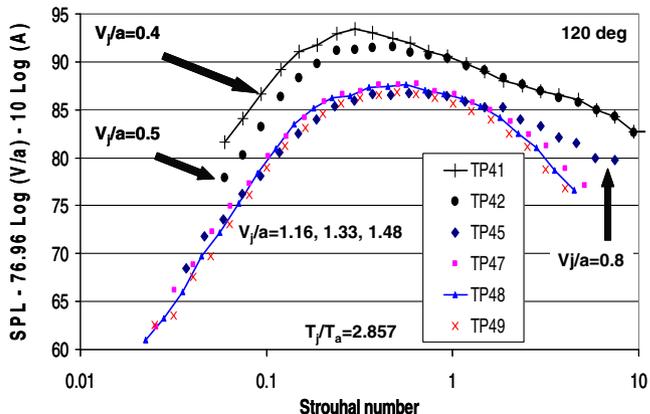

Fig. 20 Normalized spectra at 120 deg from jets with a fixed static temperature ratio of 2.857. Tanna's data.

120 deg from jets with a high fixed static temperature ratio of 2.857 are normalized; the velocity exponent has been calculated to be 7.696. First of all, there is good collapse of the spectra at the three highest velocities, $V_j/a = 1.16$, 1.33, and 1.48. As seen in Fig. 15, these spectra are not affected by rig noise and there is good collapse over the entire frequency (Strouhal number) range at this very high T_j/T_a. The spectrum for the next lower velocity, $V_j/a = 0.8$ and denoted by diamonds, has elevated levels at the highest five frequencies; this observation indicates that the rig noise has an impact for raw frequencies of ≥ 16 kHz for this V_j/a. Incidentally, this run number (TP45) corresponds to the lowest curve (denoted by dark squares) in Fig. 13. Further, a set of these four curves was presented as Fig. 22 in [9]. The spectra at two lower velocities, $V_j/a = 0.4$ and 0.5, are included here; the Mach numbers that correspond to these test points are 0.237 and 0.296, respectively. These spectra have increased sound pressure amplitudes at all the frequencies; the levels are ~6 dB higher for the lowest V_j/a of 0.4 in the low-frequency regime all the way to the spectral peak. Clearly, the rig noise has a profound impact on the spectral shape and amplitude at these very low Mach numbers. Note that this test case, TP41, is used in Fig. 12 in the identification of the two master spectral shapes for the heated and unheated jets.

To put the issue of rig noise in perspective, normalized spectra at the same radiation angle of 120 deg from jets at a fixed static temperature ratio of 2.0 from the current database are shown in
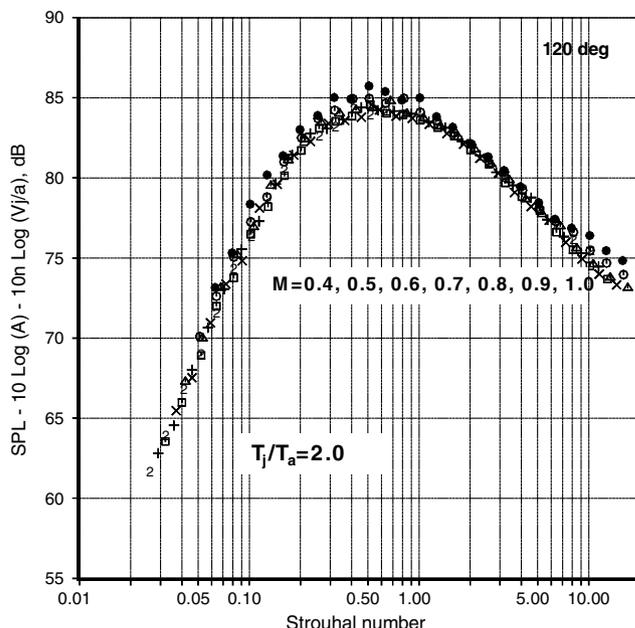

Fig. 21 Normalized spectra at 120 deg from jets with a fixed static temperature ratio of 2.0. Current data.

Fig. 21. The spectrum from the lowest Mach number jet ($M = 0.4$, $V_j/a = 0.57$), denoted by the dark circles, has slightly elevated levels, especially near the spectral peak and at the highest frequencies. Otherwise, there is excellent collapse of the spectra for the higher Mach numbers throughout the Strouhal number range. Unfortunately, data have not been acquired at lower Mach number jets in the new database. However, an examination of the entire database reveals the availability of data at lower Mach numbers (and lower V_j/a) at constant stagnation temperature ratios. A Mach 0.3 jet with $T_t/T_a = 1.8$ yields a jet velocity of $V_j/a = 0.39$. The spectra from this case and the one from an unheated jet at $V_j/a = 0.4$ are compared in Fig. 22; let us ignore the spectrum denoted by the crosses and a line for the time being. At first blush, it is tempting to conclude that the heated jet (dark circles) is ~3 dB noisier than the unheated jet (open circles) in the lower frequency regime up to the spectral peak. In the high-frequency portion of the spectra, both the jets have similar levels. Except for the difference in amplitude, ~6–7 dB versus ~3 dB, there seems to be good resemblance between this figure and Fig. 12, which was taken from Tanna et al. [5].

Does this mean that the spectral shape changes with increasing temperature for low-velocity jets? Let us investigate this issue in detail. Viswanathan [9,11] pointed out that the scaling laws can be used to check data quality. We adopt this procedure and collapse the spectra from jets at fixed $T_t/T_a = 1.8$; the normalized spectra are depicted in Fig. 23. There is excellent collapse for the jets with Mach numbers of 0.5–1.0. The $M = 0.4$ jet, denoted by the number 2, has slightly elevated levels, comparable to the mismatch seen in Fig. 21 for jets with constant $T_j/T_a = 2.0$. The effect of rig noise is more pronounced for the $M = 0.3$ jet, with a ~3 dB increase in levels in the low-frequency regime and at the spectral peak. We recognize the likelihood of misinterpreting the elevated levels as being due to rig noise and not an additional source of noise; however, we discount this possibility because we do not expect the physics that holds for a velocity range of 0.54–1.23 ($M = 0.4$–1.0) to change drastically at $M = 0.3$. Furthermore, thorough analyses carried out and reported in several publications enable the identification of the effect of rig noise and the range of affected frequencies. A similar level of contamination is observed at 125 deg for the $M = 0.3$ jet, as shown in Fig. 18 in [9]. Further, the Reynolds numbers for the $M = 0.3$ and 0.4 jets are ~213,000 and ~310,000, respectively. The Reynolds numbers for the higher Mach number jets span a range of ~405,000–1.19 × 10⁶. Thus, there are two reasons for the elevated levels at the spectral peak and at the lower frequencies: rig noise, and
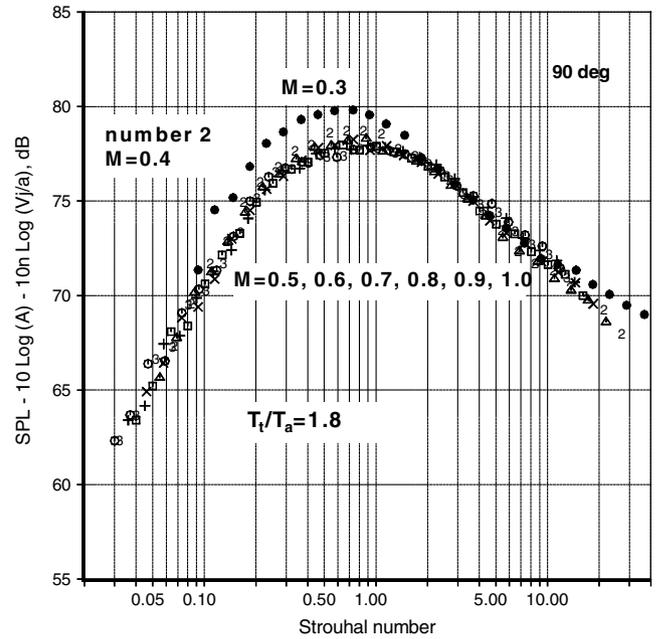

Fig. 23 Normalized spectra at 90 deg from jets with fixed $T_t/T_a = 1.8$.

effects associated with low Reynolds numbers. The magnitude of ~3 dB is comparable to the elevated levels observed in Fig. 22 for the heated jet. Therefore, the change in spectral shape in Fig. 22 is not associated with the appearance of an additional noise source.

Viswanathan [11] demonstrated that it is easier to make an accurate prediction using the scaling laws than to obtain clean measurements, especially at low jet velocities. Again, a prediction is made for $V_j/a = 0.4$ using the scaling laws; this spectrum is included in Fig. 22 and is denoted by the crosses and the line. As seen, the predicted curve is much closer to the data from the unheated jet; there is a slight increase in level of ~1 dB near the spectral peak but not the ~3 dB in the entire low-frequency region of the measured spectra, denoted by the closed circles in Fig. 22. It is also interesting that there is no drastic change in the spectral shape between the heated and unheated jets. This is not an entirely new finding: Viswanathan [10,17] established previously that the spectra from heated jets conform to the fine-scale similarity at the low radiation angles, regardless of the jet Mach number and the temperature ratio. Several examples are provided in these references. Figure 17 in [9] clearly shows this to be the case, as the normalized spectra at various V_j/a at two extreme stagnation temperature ratios of 1.8 and 3.2 have identical shapes. Finally, we show a direct comparison of the predicted spectrum with $V_j/a = 0.394$ at $T_t/T_a = 1.8$ with a comparable measurement from Tanna (TP22) in Fig. 24. Not surprisingly, the entire spectrum is higher by ~3 dB for this very low-velocity jet.

What is the reason for the observed differences in spectral shapes at low $V_j/a = 0.4$ in Fig. 12 from Tanna? The following likely scenario emerges when we weigh the evidence carefully. It is clear from Fig. 20 that the level of contamination is ~6 dB in the low-frequency regime all the way to the spectral peak for TP41. This is roughly the magnitude of the increased level observed in Fig. 12 for the heated jet in the frequency range of 200–1250 Hz. The Reynolds number for the heated jet is ~79,000; this low Reynolds number would also produce a hump near the peak (see [10]). If we account for these two effects and subtract ~6 dB, then the levels would be comparable in the low-frequency regime. The magnitude of the contamination is slightly lower, ~4 dB, at the higher frequencies in Fig. 20. The contamination in the unheated spectrum (TP2) is ~4 dB for the frequency range of 4–40 kHz, as established in Fig. 11. Both the unheated and heated jets have comparable levels over the high-frequency range, because both of them have been subjected to the same level of contamination. It should be perfectly clear now why the different spectral shapes are observed in Tanna's data: it is entirely due to the consequence of poor-quality data. We further draw
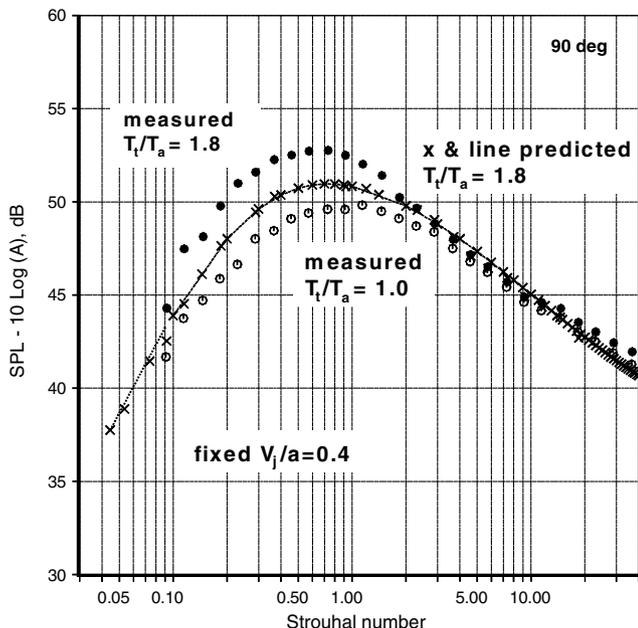

Fig. 22 Spectra at 90 deg from jets with fixed $V_j/a = 0.4$. Closed circles: $T_t/T_a = 1.8$; open circles: $T_t/T_a = 1.0$.
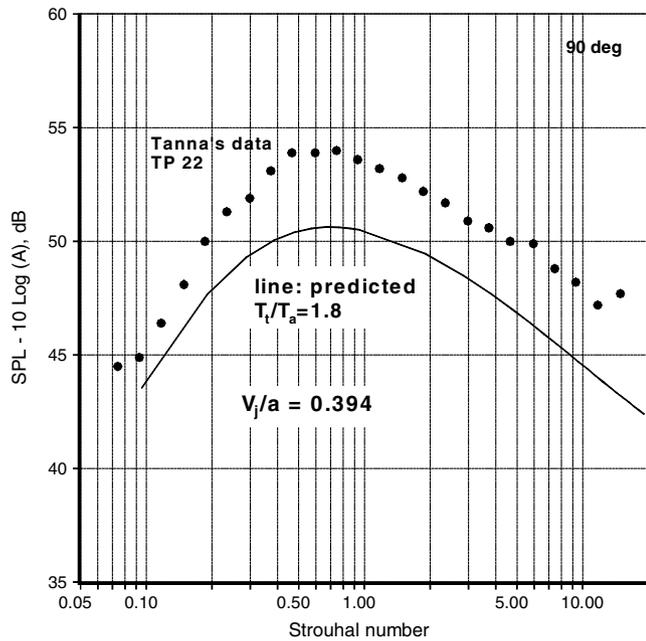
Fig. 24 Comparison of Tanna's data [13,14] with prediction from scaling laws.

attention to the drastic differences in the spectral trends at fixed jet velocity, $V_j/a = 0.8$, in Figs. 13 and 14 (and also in Figs. 18 and 19). When we examine all the evidence presented, it becomes obvious that the spectral trends noted in Tanna's data are due to erroneous measurements.

4. Aspects of Rig Noise

The most insidious effect of rig noise is the unknown magnitude of the contamination, which is a function of both the Mach number and jet temperature; the test cases shown in Fig. 18 bear out this observation. For example, the mass flow rate is the highest for the unheated jet at a fixed Mach number. For a given rig with a fixed upstream diameter for the supply plumbing, the internal velocity is consequently the highest for the unheated jet. Given that the externally generated jet noise is the lowest for the unheated jet and the internal rig noise is the highest, the entire spectrum could get corrupted. The mass flow rate decreases when a jet is heated at a fixed Mach number because of the reduced jet density due to heating. Therefore, the internal flow velocity decreases, potentially reducing the internally generated noise. However, the combustor noise becomes an issue. Though the combustor noise is generally believed to be restricted to low frequencies, it was observed by Viswanathan [20] that it could severely affect the jet spectra from 200 Hz to ~8 kHz; see Fig. 15 and the associated discussion in [20]. An attempt was also made to measure rig internal noise in [20] through the use of nozzles of different diameters. Typically, the mass flow rate for a given jet operating condition for the smaller nozzle is calculated and maintained fixed for the large nozzle as well. However, the jet exit velocity would be lower for the larger nozzle; scaling laws can be used to calculate the intensity of noise radiated by the two nozzles. The ratio of the intensities is proportional to the diameter ratio raised to a high power (equal to 2 times the velocity exponent). As shown in Fig. 13 in [20], this approach is not foolproof.

Generally, it has been found during the course of conducting aeroacoustic tests over many years by the first author that, once the jet Mach number is reduced to low values, it becomes almost impossible to acquire clean data even at very high temperatures. A typical example is shown in Fig. 29 in [10]. Spectra obtained at a high stagnation temperature ratio of 3.2 at several Mach numbers are compared; the jet velocities (V_j/a) at the lowest four Mach numbers of 0.18, 0.22, 0.25, and 0.28 are 0.32, 0.39, 0.44, and 0.49, respectively. Still, the spectral shape as well as the level for the higher

three V_j/a are completely wrong, as seen in Fig. 29b in [10]. This is in spite of the fact that accurate spectral measurements have been made from an unheated jet with $V_j/a = 0.4$. This example attests to the complex nature of contamination by rig noise. It was also shown in [10] that the velocity exponent for OAPWL drops from 7.98 to 5.9 when the contaminated data at low V_j/a are included in the calculation of the exponent, thereby providing false experimental trends to the theoreticians.

An important conclusion is drawn from the exercise: there is no such thing as a "qualitative" noise measurement. Completely incorrect spectral trends could result from poor-quality data, as exemplified by the spectral comparisons shown in Figs. 13 and 14. In addition to misleading the development of theories and scaling laws, there is a bigger danger in the evaluation of noise reduction concepts. Because the magnitude of the contamination varies with frequency, the perceived benefit of any device that alters the shape of the spectra by transferring energy from the low to high frequencies could be completely wrong. Therefore, clean measurements are absolutely vital at all angles and frequencies.

A further point should be kept in mind. If the jet rig includes improper fittings, such as steps, gaps, and screw-heads exposed to the flow, these can create tones and broadband noise of unknown magnitude at unknown frequencies. The minimum Mach number, at which meaningful measurements are possible, also varies from rig to rig and is strongly dependent on the design of the rig and the diameter of the nozzle being tested. It should also be kept in mind that, for certain combinations of Mach number and temperature, it might be possible to obtain clean data as the balance between the jet noise and rig noise could be favorable. The improper selection and design of the instrumentation system could further compound the problem, especially at high frequencies. As can be appreciated, there is no simple way of quantifying the effects of internal noise contamination. Qualification tests are absolutely vital; the current scaling laws provide a quantitative means for checking data quality.

D. Noise of Low-Velocity Jets

The preceding discussion on rig noise sets the stage for the investigation of the noise from low-velocity jets and jets at constant velocity. Apart from the scientific importance of gaining a better understanding of the physics of the noise sources, there is a practical application as well. The bypass ratios of the turbofan engines that power commercial aircraft are steadily going up, after remaining around ~5.5 for nearly 25 years. For example, the bypass ratio of the engines that power the Boeing 787 aircraft is ~10. The operating conditions for the primary jet have dropped substantially, with a Mach number of ~0.5 and a temperature ratio of ~2.7. It is imperative that accurate measurements are made and good physical models of the jet noise for prediction purposes are developed at these conditions.

Some preliminary results on jets at constant velocity, the so-called density effect, were presented by Viswanathan [10]; see Sec. 4.5 for complete details on the test conditions. To summarize, acoustic data have been obtained at six fixed values of V_j/a of 0.53, 0.62, 0.73, 0.8, 0.9, and 1.2. The stagnation temperature ratios span a range of 1.0–3.05. The OAPWL increases with temperature at the two lowest V_j/a; the OAPWL is insensitive to temperature at the two middle V_j/a; and the OAPWL decreases with jet temperature at the two highest V_j/a, though the trend is less pronounced at $V_j/a = 0.9$. Spectral characteristics are examined and their interpretations are reevaluated here in light of the scaling laws developed since [10].

The spectral variations at $V_j/a = 0.8$ and at 90 deg were already presented in Fig. 14. It was established that all the heated jets have the same spectral level from 4 to 80 kHz. Before we examine the spectral characteristics in the aft quadrant, we present results at 90 deg for the two lowest V_j/a. It should be appreciated that there is a drastic reduction in the Reynolds number for these low-velocity jets. In Fig. 25, for jets with $V_j/a = 0.62$, the jet stagnation temperature ratios span a range of 1.0–2.48 for the seven cases shown. The spectra from the heated jets, denoted by numbers, increase sequentially with increasing temperature ratio, thereby facilitating a symbolic easy
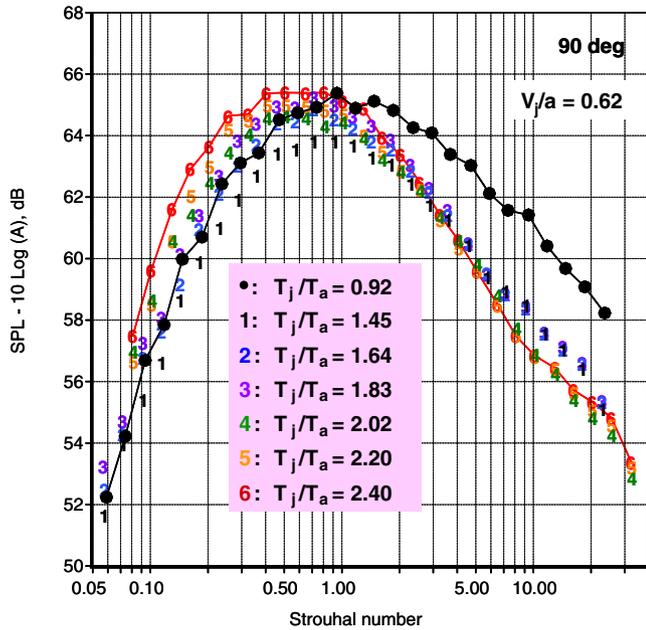
Fig. 25   Spectra at 90 deg from jets with fixed jet velocity; $V_j/a = 0.62$.

Fig. 26   Spectra at 90 deg from jets with fixed jet velocity; $V_j/a = 0.53$.

visualization of the various spectra. The spectrum from the jet at the maximum temperature is also in red. Two nozzles with diameters of 2.45 and 3.46 in. have been used to acquire the data. The spectra from the smaller nozzle are shown for the lowest four temperature ratios; the Reynolds numbers range from $\sim 1.178 \times 10^6$ to $\sim 336,000$. The spectra obtained with the bigger nozzle are used for the highest three temperature ratios; the Reynolds numbers range from $\sim 400,000$ to $\sim 297,000$. As with the spectra at $V_j/a = 0.8$ in Fig. 14, the unheated jet has higher levels over a wide range of higher Strouhal numbers from ~ 1.5. The spectral levels for the heated jets are again the same for Strouhal numbers of ≥ 2.0. The more interesting trends are observed at the lower Strouhal numbers:

1) There is no change in peak level even for the hottest jet denoted by the number 6 and a line.

2) The increase in level at the very low frequencies is ~ 2 dB.

3) The differences in levels for the lower temperatures are within ~ 1 dB of the unheated jet.

A still lower V_j/a of 0.53 is considered in Fig. 26. Again, the spectra from both nozzles are shown; the values of the Reynolds numbers range from $\sim 935,000$ for the unheated jet to $\sim 247,000$ for the jet at the highest temperature ratio of 2.42. Once again, the spectra from all the heated jets have similar levels over a wide range of higher frequencies. Interestingly, there is a 1.2 dB reduction in the peak level (and a reduction at all the frequencies) when the jet is first heated to a static temperature ratio of 1.47. With a further increase in temperature, there is a slight increase in the peak levels: 0.9 dB for the jet at $T_j/T_a = 2.23$ and 0.7 dB for the jet at $T_j/T_a = 2.42$. It is hard to attribute this trend only to heating, as the low Reynolds numbers could play a substantial role in the observed increase. Nevertheless, the maximum increase is only ~ 2 dB even for the highest temperature ratio of 2.42. Now it is established that all heated jets at fixed V_j/a have the same spectral levels at the higher frequencies in the low-to-moderate-velocity range of 0.5–0.8. At a high V_j/a of 1.2 (Fig. 19), the spectral levels are similar at the lower frequencies; there is a slight reduction of ~ 2 dB at the higher frequencies. Note that the Reynolds numbers are greater than $\sim 365,000$ for all the jets at this high V_j/a. For a deeper analysis of the spectra at low velocities, see Viswanathan [21].

The variations in spectral shapes and level are more interesting in the aft quadrant. The spectra at a fixed $V_j/a = 0.8$ at two large aft angles of 145 and 155 deg are presented in Figs. 27 and 28, respectively. All the spectra, except for the unheated case, have the same level at the lower frequencies and up to the spectral peak in Fig. 27; the level for the unheated jet is slightly lower. In the high-
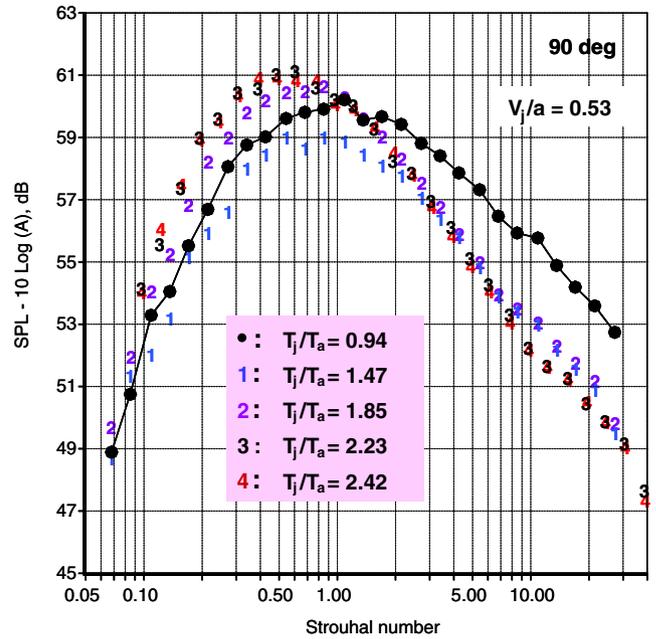
frequency regime, beyond the spectral peak, the trends are clear: the levels keep decreasing progressively with increasing temperature. In Fig. 28, the spectra for all the jets, including the unheated case, are identical in the low-frequency regime and at the spectral peak. Again, there is a clear trend of decreasing levels with temperature in the high-frequency regime, to the right of the spectral peak.

Do these trends imply that there is a reduction in the high-frequency spectral levels if a jet is heated at fixed jet velocity, as has been believed? Not necessarily. To aid the discussion, Fig. 20 in [9] is reproduced here as Fig. 29. Jets at three stagnation temperature ratios of 1.0, 1.8, and 3.2 are considered; that is, the jet temperature is increased by $\sim 80\%$ each time. Table 1 in [9] provides the jet operating conditions for the test points considered: the Mach numbers span a range of 0.3–1.0 in steps of 0.1. Attention is drawn to an important parametric variation of V_j/a: the ranges for the three temperature ratios are (0.287–0.912), (0.386–1.226), and (0.516–1.643), respectively. That is, there is significant overlap of the velocity ratios, with the jet velocities at the higher NPR for the lower temperature ratios being higher than those at the lower NPR for the higher-temperature jets. The normalized spectra at the three temperature ratios are depicted at 145 deg in Fig. 29. It is readily evident that there are three distinct families of curves, each with a unique shape, for all jet velocities within that group. For example, an examination of Table 1 in [9] indicates that the jet velocity ($V_j/a = 0.912$) for the unheated jet at an NPR of 1.89 is higher than the lowest five test points at a temperature ratio of 1.8 and the lowest three points at a temperature ratio of 3.2. Yet, the spectral shape has a narrower peak for the lower-velocity jets at higher temperatures in Fig. 29.

This figure and Fig. 19 in [9], which shows a similar plot at an angle of 125 deg, indicate that the spectral shape at a particular aft angle is controlled more by the temperature ratio than the velocity ratio. As noted by Viswanathan [9], this is a surprising result and the strong influence of the temperature ratio on spectral shape at aft angles has never been recognized in any previous study. As amply demonstrated in [9,11] and here, a particular velocity exponent, which is a function of the temperature ratio and the radiation angle, collapses the spectra over the entire frequency range from jets of all V_j/a at that particular angle. As seen in Fig. 29, the spectra get progressively narrower with increasing temperature; this is true for any jet velocity.

Let us reexamine Figs. 27 and 28; the main difference is in the low-frequency portion of the spectra, only for the unheated jet. Very recently, Viswanathan [22] demonstrated that the spectra from even
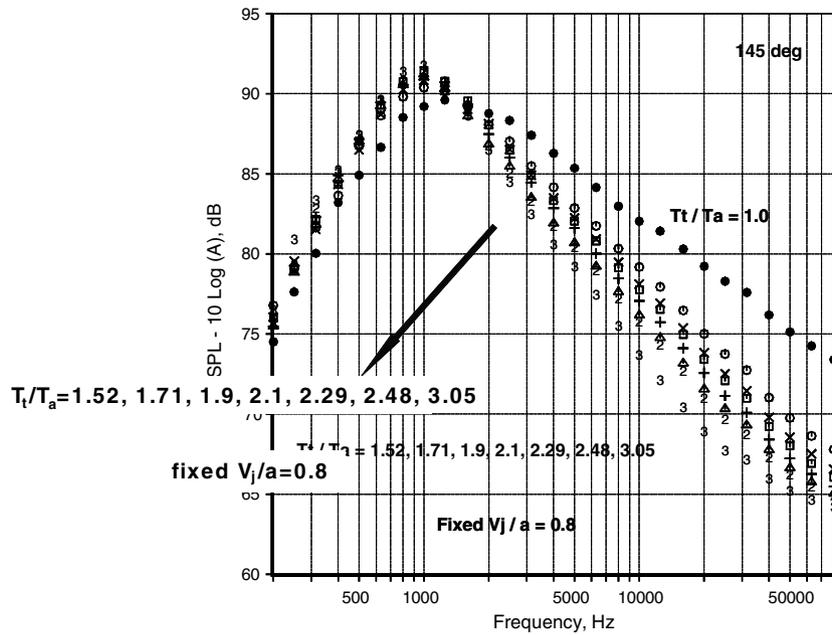
Fig. 27 Spectra at 145 deg from jets with fixed jet velocity; $V_j/a = 0.8$.

very low unheated jets eventually attain the large scale similarity (LSS) shape of [18] at angles close to the jet axis. There is a gradual progression from the broad spectral shape, say at 90 deg, to the narrower shape. The spectra from unheated jets retain the broad shape to a larger angular range from the inlet, whereas heated jets attain the more peaked shape at lower angles; see Figs. 10 and 29 for example. At 155 deg (Fig. 28), the spectrum from the unheated jet has attained the LSS shape, whereas the spectrum at 145 deg is still in the transition stage from the broad to the peaky shape. This intrinsic characteristic of jet spectra explains the trends observed in Figs. 27 and 28. These trends serve to answer the question posed earlier: the spectral shape is controlled by the jet temperature and not velocity. Therefore, it would be incorrect to say that "a reduction in the Reynolds shear stress contribution with increasing temperature" is responsible for the progressive reduction in the higher frequencies when the jet is heated at fixed velocity, as postulated by Tanna et al. [5] and many other theoreticians.

Finally, we present the spectra from jets at a fixed high velocity of 1.2 in Fig. 30. The reason for this figure is that there is a noticeable

monotonic reduction in level at the spectral peak, in addition to the higher frequencies, when the temperature is increased at this high jet velocity. At a lower V_j/a of 0.8, there is no change in the peak levels.

E. Validity of Classical Theories of Jet Noise

We now revisit the scaling laws and theoretical models of jet noise; invariably, all the classical models lead to the form given by Eq. (1). As noted in Sec. III.B in Viswanathan [9], the different models adopt different descriptions of the noise sources and several associated assumptions. Based on a given approach, either the dipole (with V^6 dependence) or the monopole (with V^4 dependence) emerged as an additional source of noise for hot jets. In all these models based on variants of Lighthill's acoustic analogy, the quadrupole source, with V^8 dependence, was thought to be the dominant source of noise, especially for isothermal and unheated jets. The coefficients in Eq. (1), A_1, B, and C, are complicated functions of the temperature ratio and the functional forms depended on the assumptions invoked. For example, in the model of Fisher et al. [2],
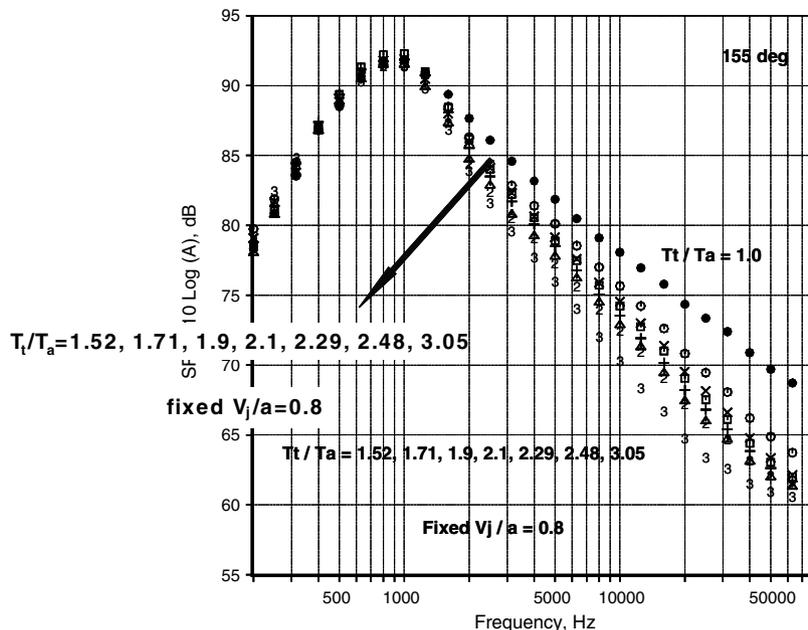

Fig. 28 Spectra at 155 deg from jets with fixed jet velocity; $V_j/a = 0.8$.
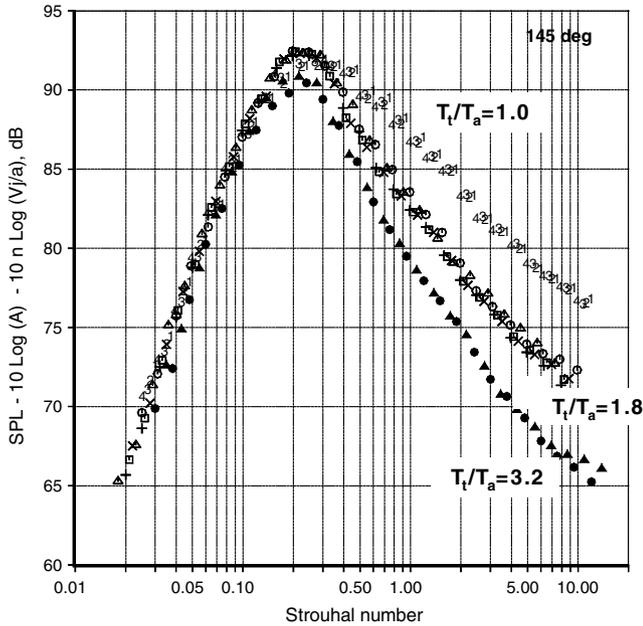
Fig. 29 Normalized spectra from jets at different velocities at 145 deg. Numbers: $T_t/T_a = 1.0$; open symbols: $T_t/T_a = 1.8$; closed symbols: $T_t/T_a = 3.2$.

$$A_1 \propto (T_j/T_a)^{-1}, \qquad B = 0, \quad \text{and} \quad C \propto (T_j/T_a)^{-1}(\ell_n(T_j/T_a))^2 \tag{4}$$

A similar choice of sources resulted in the study of [5], except that the velocity dependence for the quadrupole source was 7.5 instead of 8.0. The model of Morfey [3] favored a combination of the quadrupole and dipole sources, with

$$B \propto ((T_s - T_a)/T_s)^2, \quad \text{and} \quad C = 0 \tag{5}$$

where T_s is the source temperature in this formulation; several expressions for the source temperature have been considered in scaling spectra, as will be noted.

In the model of [2], it was suggested that the contribution from the quadrupole term decreased with increasing jet temperature. Morfey

[3] suggested that this term should be independent of temperature. His model also predicted that, at higher V_j/a, the noise from heated jets at lower frequencies should be independent of jet temperature, whereas the spectral levels at higher frequencies would diminish as $(T_j/T_a)^{-3.5}$. The model of Lilley [4] included all three noise sources, with the contribution from the different sources dependent on the jet temperature and V_j/a. It should be noted that all the models, irrespective of the final form, led to the presence of an additional noise source for heated jets. The form of the additional source depended on the treatment and manipulation of the term $p - a^2\rho$ in Lighthill's stress tensor with different flow variables.

The spectra from jets at low velocities ($V_j/a = 0.4$) and at higher velocities ($V_j/a \geq 0.8$) from Tanna's database, shown here as Figs. 12, 13, and 18, provided the rationale and the justification for most of the theories and models developed in the 1970s and early 1980s. Similar trends were observed at even lower jet velocities in the data obtained at the Institute for Sound and Vibration Research [2]. It has been convincingly established here that Tanna's data suffer from serious contamination at these jet velocities. Nevertheless, we focus our attention on two of the models, that of Tanna et al. [5] and Morfey et al. [6], and carefully examine the theoretical arguments and assumptions in support of the model development. These two studies were specifically chosen as these models attempted to tie their scaling laws to measured data, unlike most other research, which is restricted to developing variants of the acoustic analogy that result only in sets of equations. Tester and Morfey [23] provide details of the shear flow analogy model that accounts for the mean-flow interaction; this model is incorporated in [6].

Tanna et al. [5] and Morfey et al. [6] adopted the sensible practice of analyzing the data at 90 deg from isothermal jets ($T_j/T_a = 1$), for which the contribution from the dipole sources is zero by definition. The constant of proportionality for the quadrupole source was evaluated and fitted to this set of isothermal data. There are certain differences in the formulation at 90 deg in these two references, however. In [5], several variants of the source temperature were considered; these consisted of the geometric mean, the arithmetic mean, and another formula:

$$T_s/T_a = \sqrt{T_j/T_a}, T_s/T_a = (T_j + T_a)/T_a, \qquad \text{or}$$
$$T_s/T_a = 0.7((T_j/T_a) - 1) + 1 \tag{6}$$

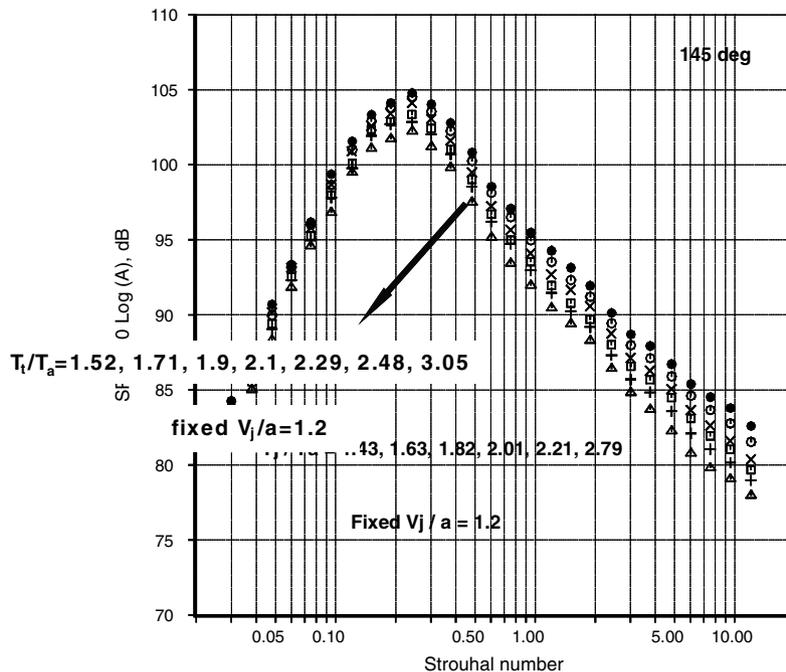The Doppler amplification factor of Lighthill and Ffowcs-Williams

Fig. 30 Spectra at 145 deg from jets with fixed jet velocity; $V_j/a = 1.2$.

[24] was also neglected; the corresponding expression for intensity at 90 deg is given by

$$I \approx \frac{(V_j/a)^8}{\left[1 + \alpha^2 M_c^2\right]^{\frac{5}{2}}} \tag{7}$$

The second term in the denominator was dropped for simplicity. Also, the plain Strouhal number was used in [5] for scaling frequency.

Morfey et al. [6] developed a more elaborate form for the source temperature that was a function of the Strouhal number as follows (see Appendix 2 of [6] for complete details):

$$(T_s/T_a)(S_m) - 1 = ((T_s/T_a)(\infty) - 1)\left\{0.98 + 0.073S_m^{-2}\right\}^{-0.25} \tag{8}$$

where S_m is the modified Strouhal number based on geometric acoustics and is defined as follows:

$$S_m = SD_m \tag{9}$$

where S is the regular Strouhal number, and D_m is the modified Doppler factor:

$$D_m^2 = \{1 - D_s U_c \cos\theta_s/c_s\}^2 + (U_j D_s/c_s)^2\left\{\alpha^2\sin^2\theta_s + \beta^2\cos^2\theta_s\right\} \tag{10}$$

The subscript s denotes any quantity with the value at the source. D_s is the Doppler factor based on source velocity U_s, and U_c is the convective velocity, usually assumed to be $\sim 0.65 - \sim 0.7\ U_j$. At 90 deg, the preceding expressions simplify, because cos (90) is zero and sin (90) is unity. A modified Strouhal number, given by the product of the regular Strouhal number and the modified Doppler factor, was also used to scale the frequency. The optimum value of α was determined to be 0.2 from a detailed analysis of the isothermal data. At other angles, an additional parameter β appeared in the expression for the modified Doppler factor.

In [6], the following expression for the noise intensity was used:

$$I \propto (T_s/T_a)^{-1}(a_s/a)^{-4}(V_j/a)^8(D_m)^{-9} \tag{11}$$

For isothermal jets, the source temperature and the speed of sound in the jet are equal to their values in the ambient medium. Note the drastic difference in the exponent for the Doppler amplification factor; see [6] for more details.

Having thus established the scaling and prediction relationship for the quadrupole source for the isothermal cases, Tanna et al. [5] and Morfey et al. [6] proceeded to test their formulation against data from heated jets in Tanna's database. They discovered that the predicted contributions from the quadrupole source alone were higher than the measured data from hot jets. This predicament is, of course, inconvenient, because in addition to the scaling for the quadrupole source being incorrect there is no room for the presence of an additional source. However, different approaches were adopted in Tanna et al. [5] and Morfey et al. [6]. Tanna et al. [5] reasoned that their original assumption of the two sources being completely uncorrelated was not quite correct and introduced a correlation coefficient, which was set to 1.0. Though this approach was more satisfactory at lower jet velocities, there was a clear overestimation at the lower frequencies for high-Mach-number jets at high temperature ratios. To overcome this difficulty, the source temperature was modified to include a function that depended on jet Mach number as follows:

$$\frac{T_s}{T_a} \approx \frac{0.7[1 + 0.2M^2]\frac{T_j}{T_a} + 0.3}{(1 + 0.1M^2)} \tag{12}$$

At higher frequencies, again there was overestimation from the scaling laws, especially when the jet temperature was significantly different from the ambient values. It was speculated that there was a

"negative source term, in antiphase with the Reynolds shear stress term ($\rho\ v_i\ v_j$)."

Morfey et al. [6] abandoned the idea of the radiation from the quadrupole being temperature independent, as posited in [3], and suggested that the problem with the overprediction by the quadrupole alone could be overcome by allowing the empirical variables α and β to vary with the source temperature ratio:

$$\alpha = \alpha_0(T_s/T_a)^p, \quad \text{and} \quad \beta = \beta_0(T_s/T_a)^q \tag{13}$$

The coefficients α_0 and β_0 were assigned the values of 0.2 and 0.4, respectively, as optimized for the isothermal jets. The values for the two new tunable constants, p and q, were estimated to be 0.6 and 0.2, respectively. There is no justification for these ad hoc fixes, introduced mainly to overcome the observed shortcomings. The underlying fundamental issues with the proposed model need to be addressed if the model is to be valid.

The thought process involved in the development of the scaling laws is interesting, if only for the fact that both studies attempted to fit the same data of Tanna. In one model, the additional source was assumed to have a V^4 dependence, in the other, a V^6 dependence. Because the velocity exponents for the sources were fixed, the multiplicative constants that are functions of the temperature ratio had to be tailored suitably. Disparate arguments and associated assumptions with suitable empirical constants were invoked in each. Morfey et al. [6] chose to adopt the source temperature, etc., as a function of the frequency. Presumably, this step provides the flexibility to tune the coefficients as necessary to fit the data. However, this step also destroys any semblance of a universal scaling law that is applicable to an entire spectrum at a particular radiation angle; perhaps this is the most objectionable feature of these scaling laws in which different parts of the spectra require different assumptions.

It is clear from Sec. III.C that there is no sufficiently accurate experimental basis for these theories, because Tanna's database suffers from extraneous contamination over a wide range of frequencies. For example, there is absolutely no variation in level in the high-frequency portion of the spectra for jets at a constant V_j/a of 0.8; see Figs. 13 and 14. We recognize that the theoreticians were misled by incorrect data and sympathize with their attempts to develop theories based on bad data, as has become clear in this study. Moreover, they did not have the benefit of the current database. However, it should be noted that uncritical acceptance of data that seemed to support the prevailing views on jet noise, based on extensions of the acoustic analogy, played a major role in the direction of research in the 1970s and early 1980s. For example, if a theory suggests that the reduction of the high-frequency levels is a function of, say, $(T_j/T_a)^{-3.5}$, and there is evidence to that effect in the measurements as seen in Fig. 13, then one is perhaps disinclined to doubt the data. The pitfalls associated with using bad data to develop theories are clear from the preceding discussion.

IV. Conclusions

A thorough investigation of the role of static and stagnation temperature ratios in correlating jet noise has been carried out. An extensive database of high-quality jet noise was used by Viswanathan [9,10] to establish the jet temperature ratio, in addition to the jet velocity V_j/a, as an independent controlling parameter of jet noise. The original database was restricted to jets at constant stagnation temperature ratios; a supplemental database with jets at constant static temperature ratios has been created. The entire database allows the critical examination of the variation of the spectral characteristics at both fixed temperature ratios. Fundamental to the scaling laws developed here is the recognition that the jet sound power (or OAPWL) does not follow exactly the eighth-power velocity law, but has a weak dependence on the jet stagnation temperature ratio. Similarly, the variation of noise intensity (or OASPL) with jet velocity at every radiation angle is a function of the jet temperature ratio. With the explicit identification of the two independent parameters, it is possible to collapse the entire spectra

from jets at various V_j/a, but at a fixed temperature ratio, either static or stagnation. Furthermore, the excellent quality of the acoustic data is highlighted once again with the perfect collapse of the spectra over the entire measured frequency range of 200 Hz to 80 kHz. The velocity exponent for scaling jet noise is then defined uniquely for each angle and temperature ratio. The stagnation temperature ratio appears to provide a slightly tighter collapse of the spectra, though not to an appreciable degree.

The variation of the velocity exponent for jets at constant T_j/T_a exhibits the same trends seen for jets at constant T_t/T_a: the values are low in the forward quadrant and increase progressively with inlet angle. Moreover, there is a monotonic reduction in the values with increasing temperature at the lower radiation angles. Once again, it has been demonstrated that the Strouhal number without the Doppler factor collapses the spectra in the aft quadrant. Spectra from jets at higher V_j/a have been measured; the analyses of these spectra indicate that effects associated with nonlinear propagation extend to lower radiation angles as V_j/a is increased.

Tanna's database has been used in the development of scaling laws and jet noise theories since the early 1970s; spectral trends from this database have provided the rationale and the justification for many of these theoretical approaches. A careful assessment of the quality of Tanna's data, both at unheated and heated conditions, has been made through direct comparison with measured data and the use of the current scaling laws. It has been established unambiguously that the high-frequency portion of the spectra from unheated jets at all subsonic Mach numbers have elevated levels due to noise contamination. The degree of contamination is a function of the jet Mach number, with the lower-Mach-number jets affected more. The affected frequency range is also a function of Mach number and is seen to span the entire range of 4–40 kHz, the maximum measured frequency. Similarly, even spectra from heated jets at lower static temperature ratios (up to ≈ 1.82) but at high subsonic M have been found to be corrupted.

The noise from jets at very low jet velocities has been examined for two good reasons: their scientific importance and practical application in the new engines. The bypass ratios of turbofan engines that power commercial aircraft are steadily going up, and the operating conditions for the primary jet have dropped substantially, with a Mach number of ~ 0.5 and a temperature ratio of ~ 2.7. It is imperative that accurate measurements are made and good physical models of the jet noise for prediction purposes are developed at these conditions. It is established that there is no change in spectral shape with heating, consistent with the trends presented in [10,17]. The two supposedly different spectral shapes observed in Tanna's data are a direct consequence of varying levels of contamination by rig noise for jets at different temperature ratios. This point was reinforced by comparing spectra at the same fixed jet velocity but at different temperatures from the databases of Tanna and Viswanathan [10]. Thus, there is no basis for many of the conclusions drawn from Tanna's data, which were used extensively in the development of theoretical models. It is a pity that the eminent theoreticians were misled by bad data; uncritical acceptance of experimental data, however supportive of a particular point of view, could lead to erroneous theories and scaling laws.

Finally, the scaling laws developed in [9] and here can be simply written as follows:

$$\text{SPL}\,(\theta, \text{St}) = F(\theta, \text{St}, (T_t \text{ or } T_j)/T_a)[V_j/a]^n$$

$$n = n(\theta, (T_t \text{ or } T_j)/T_a)$$

It is clear that this form is simple, elegant, and does not involve any adjustable constants whatsoever. As such, this formulation is vastly superior to the classical theories based on the summation of contributions from quadrupoles, dipoles, and monopoles, in which complicated temperature dependence with numerous assumptions and ad hoc functions are introduced. The fundamental difference in the two approaches is that the velocity exponent here, rather than the multiplicative functions for these source terms, is a function of the temperature ratio. Fresh thinking on the sources of jet noise and new

theories that account for the primacy of the jet temperature ratio are clearly needed.

An important conclusion is also drawn from this study: there is no such thing as a qualitative noise measurement. Completely incorrect spectral trends could result from poor-quality data, as exemplified by the spectral comparisons shown in Figs. 13 and 14. In addition to misleading the development of theories and scaling laws, there is a bigger danger in the evaluation of noise reduction concepts. Because the magnitude of the contamination varies with frequency, the perceived benefit of any device that alters the shape of the spectra by transferring energy from the low to high frequencies could be completely wrong. Therefore, clean measurements are absolutely vital at all angles and at all frequencies.

Lilley [25], in his review article, has this closing remark: "*Finally, the importance of good, reliable, and accurate experimental data in all studies of aerodynamic noise is stressed. At best the theoretical work can only assist in providing a suitable framework in which to analyze the results and the presentation of the experimental data for prediction purposes.*" This truism is timeless and always worth remembering.

References

[1] Lighthill, M. J., "On Sound Generated Aerodynamically: I. General Theory," *Proceedings of the Royal Society of London, Series A: Mathematical and Physical Sciences*, Vol. 211, 1952, pp. 564–581.
doi:10.1098/rspa.1952.0060

[2] Fisher, M. J., Lush, P. A., and Harper Bourne, M., "Jet Noise," *Journal of Sound and Vibration*, Vol. 28, No. 3, 1973, pp. 563–585.
doi:10.1016/S0022-460X(73)80040-9

[3] Morfey, C. L., "Amplification of Aerodynamic Noise by Convected Flow Inhomogeneities," *Journal of Sound and Vibration*, Vol. 31, 1973, pp. 391–397.
doi:10.1016/S0022-460X(73)80255-X

[4] Lilley, G. M., "Aerodynamic Noise," *Noise Mechanisms*, CP-131, AGARD, Neuilly-sur-Seine, France, 1974, pp. 13.1–13.12.

[5] Tanna, H. K., Dean, P. D., and Fisher, M. J., "The Influence of Temperature on Shock-Free Supersonic Jet Noise," *Journal of Sound and Vibration*, Vol. 39, No. 4, 1975, pp. 429–460.
doi:10.1016/S0022-460X(75)80026-5

[6] Morfey, C. L., Szewczyk, V. M., and Tester, B. J., "New Scaling Laws for Hot and Cold Jet Mixing Noise Based on a Geometric Acoustics Model," *Journal of Sound and Vibration*, Vol. 61, No. 2, 1978, pp. 255–292.
doi:10.1016/0022-460X(78)90007-X

[7] Goldstein, M. E., "An Exact Form of Lilley's Equation with a Velocity Quadrupole/Temperature Dipole Source Term," *Journal of Fluid Mechanics*, Vol. 443, 2001, pp. 231–236.
doi:10.1017/S002211200100547X

[8] Goldstein, M. E., "A Unified Approach to Some Recent Developments in Jet Noise Theory," *International Journal of Aeroacoustics*, Vol. 1, Jan. 2002, pp. 1–16.
doi:10.1260/1475472021502640

[9] Viswanathan, K., "Scaling Laws and a Method for Identifying Components of Jet Noise," *AIAA Journal*, Vol. 44, No. 10, Oct. 2006, pp. 2274–2285.
doi:10.2514/1.18486

[10] Viswanathan, K., "Aeroacoustics of Hot Jets," *Journal of Fluid Mechanics*, Vol. 516, Oct. 2004, pp. 39–82.
doi:10.1017/S0022112004000151

[11] Viswanathan, K., "Improved Method for Prediction of Noise from Single Jets," *AIAA Journal*, Vol. 45, No. 1, 2007, pp. 151–161.
doi:10.2514/1.23202

[12] Viswanathan, K., "Does a Model Scale Nozzle Emit the Same Jet Noise as a Jet Engine?" *AIAA Journal*, Vol. 46, No. 2, 2008, pp. 336–355.
doi:10.2514/1.18019

[13] Tanna, H. K., "An Experimental Study of Jet Noise. Part I: Turbulent Mixing Noise," *Journal of Sound and Vibration*, Vol. 50, No. 3, 1977, pp. 405–428.
doi:10.1016/0022-460X(77)90493-X

[14] Tanna, H. K., Dean, P. D., and Burrin, R. H., "The Generation and Radiation of Supersonic Jet Noise. Volume III. Turbulent Mixing Noise," U.S. Air Force Aero Propulsion Laboratory Technical Report AFAPL-TR-76-65, 1976.

[15] Viswanathan, K., "Instrumentation Considerations for Accurate Jet Noise Measurements," *AIAA Journal*, Vol. 44, No. 6, June 2006,

pp. 1137–1149.
doi:10.2514/1.13518

[16] Shields, F. D., and Bass, H. E., "Atmospheric Absorption of High Frequency Noise and Application to Fractional-Octave Band," NASA CR 2760, 1977.

[17] Viswanathan, K., "Analysis of the Two Similarity Components of Turbulent Mixing Noise," *AIAA Journal*, Vol. 40, No. 9, Sept. 2002, pp. 1735–1744.
doi:10.2514/2.1878

[18] Tam, C. K. W., Golebiowski, M., and Seiner, J. M., "On the Two Components of Turbulent Mixing Noise from Supersonic Jets," AIAA Paper 96-1716, 1996.

[19] Viswanathan, K., "Recent Advances in Jet Noise Suppression," *International Symposium on Recent Advances in Aeroacoustics and Active Flow-Combustion Control*, Jan. 2005.

[20] Viswanathan, K., "Jet Aeroacoustic Testing: Issues and Implications," *AIAA Journal*, Vol. 41, No. 9, 2003, pp. 1674–1689.
doi:10.2514/2.7313

[21] Viswanathan, K., "Mechanisms of Jet Noise Generation: Classical Theories and Recent Developments," *International Journal of Aeroacoustics*, Vol. 8, No. 4, 2009, pp. 355–408.

[22] Viswanathan, K., "Investigations of Noise Source Mechanisms in Subsonic Jets," *AIAA Journal*, Vol. 46, No. 8, 2008, pp. 2020–2032.
doi:10.2514/1.34471

[23] Tester, B. J., and Morfey, C. L., "Developments in Jet Noise Modelling —Theoretical Predictions and Comparisons with Measured Data," *Journal of Sound and Vibration*, Vol. 46, No. 1, 1976, pp. 79–103.
doi:10.1016/0022-460X(76)90819-1

[24] Ffowcs-Williams, J. E., "The Noise from Turbulence Convected at High Speed," *Philosophical Transactions of the Royal Society of London, Series A: Mathematical and Physical Sciences*, Vol. A255, April 1963, pp. 469–503.
doi:10.1098/rsta.1963.0010

[25] Lilley, G. M., "Jet Noise Classical Theory and Experiments," *Aeroacoustics of Flight Vehicles: Theory and Practice. Volume 1: Noise Sources*, edited by Harvey Hubbard, NASA, RP 1258, Aug. 1991, pp. 211–289.

C. Bailly
Associate Editor